©2018

Julia Bolanle Olayanju

UNDERSTANDING THE ANTI-CANCER ACTIVITIES OF MORINGA

ISOTHIOCYANATES IN BREAST CANCER CELLS

By

JULIA BOLANLE OLAYANJU

A dissertation submitted to the

School of Graduate Studies

Rutgers, The State University of New Jersey

In partial fulfilment of the requirements

For the degree of

Doctor of Philosophy

Graduate Program in Microbiology Molecular Genetics

Written under the direction of

Dr. Bing Xia

And approved by

New Brunswick, New Jersey

May 2018

ABSTRACT OF THE DISSERTATION

UNDERSTANDING THE ANTI-CANCER ACTIVITIES OF MORINGA

ISOTHIOCYANATES IN BREAST CANCER CELLS

By JULIA BOLANLE OLAYANJU

DISSERTATION DIRECTOR:

BING XIA

Isothiocyanates (ITCs) are a class of naturally occurring compounds shown to have anti-cancer activities and promising chemopreventive prospects. *Moringa oleifera* (MO), a cruciferous vegetable widely cultivated in the tropics, has been used by locals to treat different diseases for centuries. Moringa Isothiocyanates (MIC) is produced from *MO* when the four unique sugar-modified aromatic glucosinolates it contains are hydrolyzed in a reaction catalyzed by myrosinase. In this study, we evaluated the efficacy of MIC on 9 different breast cancer cell lines and found it to be a potent anti-cancer agent. Interestingly, two of the most sensitive cells lines to MIC, BT474 and HCC1954, were both positive for HER2. HER2 is amplified in up to 30% of breast cancers and is positively correlated with poor prognosis in patients.

We hypothesized that HER2 overexpression induces hypersensitivity to MIC in breast cancer cells. Our studies using MCF7 and MDA-MB-231 with and without HER2 overexpression further confirmed the correlation between HER2 overexpression and hypersensitivity to MIC. To understand why increased sensitivity to MIC was observed in HER2+ breast cancer cell lines as compared to HER2- cell lines, intracellular levels of reactive oxygen species (ROS) was

examined. Higher basal intracellular ROS levels were observed in HER2+ cell lines compared to HER2- ones.

We also hypothesized that the anti-cancer activity of MIC may involve an ROS regulatory pathway. Indeed, we found that MIC clearly regulates NRF2 and KEAP1 expression in multiple breast cancer cell lines. Additionally, MIC also triggers changes in intracellular ROS levels in a cell line-dependent manner, suggesting that MIC adopts different mechanisms of action in different breast cancer cell lines. Our work shows that MIC may open new frontiers in breast cancer prevention and therapy, particularly for those with HER2 amplification.

Dedication

This dissertation is dedicated

To the loving memory of my Dad (Julius O Eniola), who loved me unconditionally and instilled so much confidence in me.

&

To my mum (Funke Eniola), who believes in me, always encourages me to reach for more and stay the course no matter what

ACKNOWLEDGEMENT

young age you have all been a voice of influence and support, I will forever be grateful to you.

Table of Contents

List Of Figures

List of Tables

Title	Page Number

Chapter 1

General Introduction to Isothiocyanates

1.1.1   Moringa oleifera

Moringa oleifera (MO) is a cruciferous plant native to India, and regions of Pakistan (26). The plant belongs to the genus *Moringa which has 13 species*, the family *Moringaceae*. MO is a popular staple in different parts of the world. While some species are native to parts of India and Pakistan, others are native to Madagascar and Northeast Africa (18).

MO has been used traditionally to treat different types of diseases. In countries like Benin, it is used to combat malnutrition (39), and Type 1 and Type 2 diabetes respectively. MO has been reported to be rich in minerals (39), in vitamins such as folic acid, nicotin and in phytochemicals (49). Phytochemicals found in MO include anthraquinones, saponins and glycerol-1-9-octadecanote (6). GC-MS Analyses by Al-Asamari and colleagues show that the main compounds with potential anti-tumor properties in *MO* extracts are: Hexadecanoic acid, eugenol and isothiocyanates.

Different preclinical studies have shown that *MO* leaf extracts show significant medicinal promise. Waterman and colleagues synthesized MIC-1 (4-[α-L-rhamnosyloxy]benzyl) isothiocyanates) and MIC-4 (4-O-acetyl -α-L-rhamnosyloxy]benzyl) isothiocyanates from fresh MO leaves using a 1:5 leaves weight to water ratio. These isothiocyanates was reported to significantly reduce the gene expression of inflammatory biomarkers specifically the expression of iNOS and IL-1β at 1 and 5 µM respectively, showing the potential of isothiocyanates to reduce inflammation associated with chronic diseases. Studies to explore the anti-obesity and anti-diabetic effects of MIC-1, show that

isothiocyanates inhibits gluconeogenesis, which affects insulin sensitivity and signaling (79). MO extract rich in isothiocyanates (38.9% MIC content) has also been shown to reduce symptoms of ulcerative colitis in mice (88). Working with SH-SY5Y human neuroblastoma cells, 4-[α-L-rhamnosyloxy] benzyl) isothiocyanates) complexed with alpha-cyclodextrin was shown to have strong anti-proliferative activities (73). Studies by Al-Asamari et al, 2015 showed that the leaf extracts from *MO* inhibit growth in breast and colorectal cancer cells. Jung et al, 2014 also reported the anti-cancer properties of *MO* leaf extract. Berkovich et al, 2013 showed the anti-cancer activity of *MO* extract in pancreatic cancer. Using 3 different pancreatic cancer cells, they showed the dose-dependent effect of *MO* extract on the different types of pancreatic cancer cell lines, inhibiting their growth. All these studies support the fact that MO extract has significant medicinal value

1.1.2 Glucosinolates & Isothiocyanates metabolism

Isothiocyanates are sulphur-containing compounds found in cruciferous vegetables in their precursor form (glucosinolate). There are different types of glucosinolates found in a wide array of crucifers (figure 1.
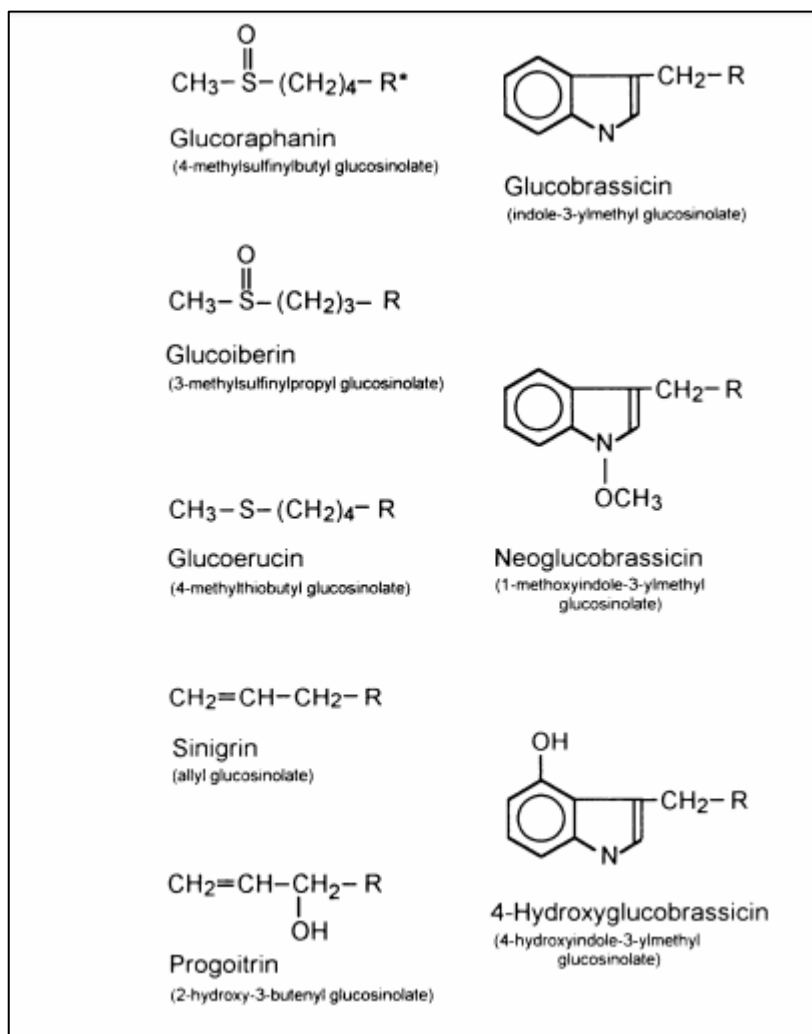
Figure 1: Glucosinolates: structures of glucosinolates commonly found in crucifers. Image adapted from Shapiro et al. 1998

Isothiocyanates are synthesized by the hydrolysis of glucosinolates when the intact plant is disrupted. The disruption of the plant exposes the glucosinolates to the enzyme myrosinase: a catalyst for the hydrolysis of glucosinolates (18). Both glucosinolates and myrosinase exist in different compartments an intact plant; they are only exposed to one another when the plant is disrupted either by chewing or blending (figure 2) (18). Various metabolites are formed when myrosinase catalyzes the hydrolysis of these glucosinolates. The products of the

hydrolysis that occurs are: isothiocyanates, indole-3-carbinols, nitriles and oxazolidine-2-thiones depending on the side chains available to the intermediate formed after the hydrolysis of glucosinolates (Figure 3) (5). The bioavailability of the isothiocyanates varies with processing of the vegetable, since processing affects the stability of myrosinase. If the cruciferous vegetable is cooked, the enzyme myrosinase is denatured and intestinal microbes later hydrolyze glucosinolates (5, 18). Protocol for isothiocyanate synthesis varies among investigators.
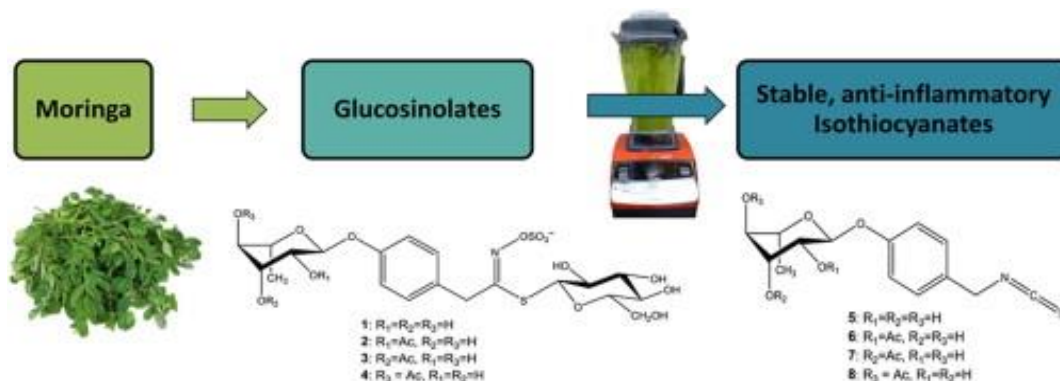
Figure 2: Moringa isothiocyanate synthesis: Blending MO plant leads to a myrosinase-catalyzed hydrolysis of glucosinolates to form isothiocyanates. Image Adapted from Waterman et.al 2015

Moringa Isothiocyanates used in this study is (4-[α-L-rhamnosyloxy]benzyl) isothiocyanates) was prepared to 98% purity following the protocol described in (80).
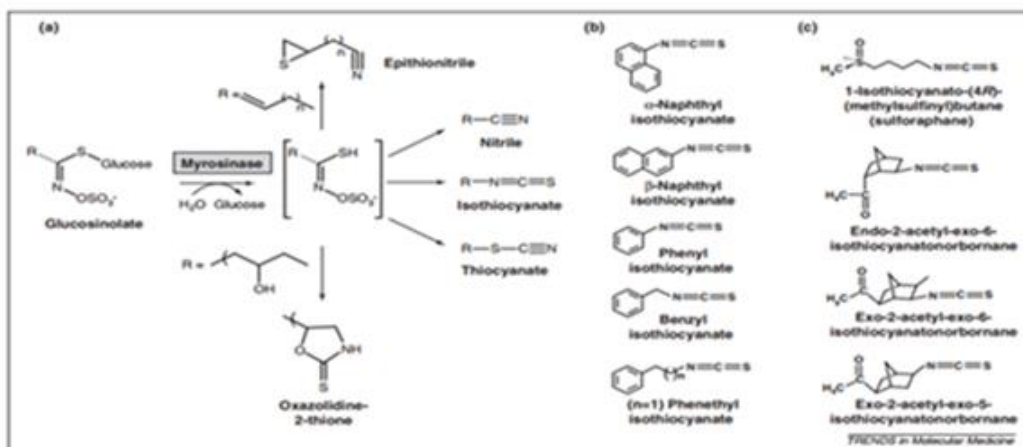
Figure 3: Mechanism of Isothiocyanates synthesis: (a) Chemical reaction showing hydrolysis of glucosinolates in the presence of the enzyme myrosinase. Different possible products that can be formed from glucosinolate hydrolysis catalyzed by myrosinase. Different products can be formed depending on the glucosinolates side chain and reaction conditions. Products that can be formed include nitriles, thiocyanites, epithionitriles, oxazolidine-2-thiones, and isothiocyanates. (b) Chemical structures of aromatic isothiocyanates. (c) Chemical structures of isothiocyanate, sulphoraphanes and its analogs. *Image adapted from Dinkova-Kostava and Kostov 2012*

Since Robiquet and Boutron isolated the first isothiocyanates in 1831, more than 120 isothiocyanates have been isolated. Different types of isothiocyanates have been studied extensively. The popular ones are: Phenyl ethyl isothiocyanates (PEITC), Sulforaphane (SFN), benzyl isothiocyanates (BITC), and allyl isothiocyanates (AITC), their respective cruciferous vegetables sources is shown in table 1. These isothiocyanates have also been reported to show anti-cancer properties in several studies.
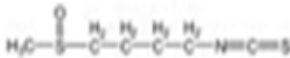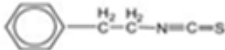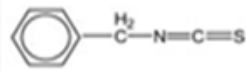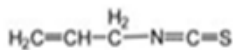
Glucosinolates	Isothiocyanate	Food sources
Glucoraphanin	Sulphoraphanes	Brussel sprouts
Gluconasturtin	Phenyl ethyl Isothiocyanates	Watercress
Glucoraphanin	Benzyl isothiocyanates	Garden cress
Sinigrin	Allyl-isothiocyanate	Horseradish mustard

Table 1: Structures of Different Isothiocyanates: glucosinolate precursor for each isothiocyanates and their respective food sources

1.1.3 Anti-cancer activities of Isothiocyanates

Epidemiological studies show that dietary consumption of cruciferous vegetables reduces the risk of breast, lung and colon cancer (3, 7, 21) Xiao and colleagues (2003) showed that allyl isothiocyanates (AITC) inhibits growth of androgen independent (PC-3) and androgen dependent (LNCaP) cultured human prostate cancer cells. This study also established a correlation between the inhibition of growth of PC-3 cells in the presence of AITC and G2/M cell accumulation coupled with apoptosis. Reduction in the protein levels of CDK1, CDC25B and CDC25C was observed after treating PC-3 and LNCaP cells with AITC for 24 hours

Gupta and Srivastava 2012 showed that overexpressing HER2 increased sensitivity to PEITC while silencing of HER2 reduced the effects of PEITC. This

study also showed that PEITC induced apoptosis and ROS at a higher level in HER2 overexpressing cells than in parental cells (27).

Sulphoraphanes is another well-studied isothiocyanate with anti-cancer activities; it was shown that SFN acted synergistically with cisplatin to inhibit gastric cancer cells growth, MGC803, BGC823 (GC) viability. According to the study, 10 μM of SFN did not inhibit gastric cancer cell viability; neither did low dose of cisplatin (2 μM) (77). However, combining 10 μM SFN and 2 μM cisplatin inhibited the growth in gastric cancer cell lines MGC803, BGC823 (77).

Benzyl isothiocyanate (BITC), has been studied by different laboratories attempting to understand its anti-cancer activities on different types of cancer. BITC inhibits the growth of human mammary cancer cells grafted into mice (78). Boreddy and colleagues treated mice with BxPC-3 tumor xenografts with benzyl isothiocyanates and observed a 43% reduction in tumor growth. This study also showed a reduction in phosphorylation of PI3K, AKT, PDK, FOXO3a, FOXO1 and mTOR in response to treatment with BITC.

Even though studies have reported the antitumor effects of MO extract, studies involving moringa isothiocyanates are few. Our objective in this study is to understand the activities of moringa isothiocyanates (MIC-1) in breast cancer cells.

1.2 Materials and Methods

1.2.1 Cell culture

Human breast carcinoma cell lines MCF-7, MDA-MB-231, MDA-MB-436, MDA-MB-468, BT-474, HCC-1954, T47D, Hs578T and non-tumorigenic cell line MCF10A were retrieved from the Xia lab frozen stock collection (Table 2). The carcinoma cell lines were maintained in Gibco™ Dulbecco's Modified Eagle Medium: Nutrient Mixture F-12 (DMEM-F12) which was supplemented with 10% fetal bovine serum (FBS) and 1% penicillin. MCF-10A cell lines was maintained in DMEM/F12 supplemented with 5% horse serum, 1mg/ml EGF, 1mg/ml hydrocortisone, 1 mg/ml cholera toxin, 10 mg/ml insulin and 1% penicillin.

1.2.2 Cell Viability Assay

Cells were prepared for cell sensitivity assay by plating in 96 well plates at a density of 2000 cells per well. The cells were allowed to grow overnight before treatment with PEITC or MIC at different concentrations. PEITC (99% purity and a molecular weight of 163.2) was purchased from Sigma Aldrich, ST Louis, MO, USA while MIC-1 was a generous gift from Dr. Ilya Raskin's lab at Rutgers University New Brunswick. Cells were treated with different concentrations of PEITC (0.01 μM to 10 μM) and MIC-1 (0 to 1 μM) respectively and allowed to incubate for 72 hours before cell viability measurement. Cell viability was measured using CellTiter Glo luminescent cell viability assay (Promega).

Cell Line	Morphology	Histology	Source	Classification	ER	PR	HER2	Mutant genes
MCF10A	Epithelial	Fibrocystic	PT	Basal B	-	-	-	CDKN2A loss
MCF7	Epithelial	IDC	PE	Luminal	+	+	-	CDKN2A, PIK3CA
T47D	Epithelial	IDC	PE	Luminal	+	+	-	TP53, PIK3CA
BT-549	Polymorphic	IDC	PT	Basal B	-	-	-	TP53 (R249S), PTEN, RB1
Hs578T	Mesenchymal-like	CS	PT	Basal B	-	-	-	TP53, CDKN2A
MDA-MB-231	Mesenchymal-like	AC	PE	Basal B	-	-	-	TP53, BRAF, CDKN2A, KRAS
MDA-MB-436	Mesenchymal like	AC	PE	Basal B	-	-	-	TP53, BRCA1, RB1
MDA-MB-468	Epithelial	AC	PE	Basal A	-	-	-	TP53 (R273H), PTEN, RB1, SMAD4
BT-474	Epithelial	IDC	PT	Luminal	+	+	+	TP53, PIK3CA
HCC1954	Epithelial	IDC	PT	Basal	-	-	+	TP53, PIK3CA
SKBR3	Epithelial	IDC	PE	Luminal	-	-	+	TP53 (R175H)
MDA-MB-453	Epithelial	CS	PE	-	-	-	+	CDH1 PIK3CA
ZR-75-1	Epithelial	CS	MT	Luminal	+	+	+	PTEN

Table 2: List of Breast Cancer Cell lines: Showing the different cell lines used in the study along with gene mutation, morphology and histology information. Abbreviations: IDC = invasive ductal carcinoma, CS =carcinoma squamous, AC = adenocarcinoma, PT = Primary tumor, PE = Pleural effusion, MT= metastatic site, ER = Estrogen Receptor, PR= Progesterone receptor

1.3 Results and discussion

1.3.1 Moringa Isothiocyanates inhibits breast cancer cell proliferation

Studies by Jung and colleagues show the inhibitory effect of *Moringa oleifera* leaf (MOL) extract on different cancer cells (119). However, since MOL contains other compounds, some of which have been reported to exhibit anti-cancer activities (1) it is important to evaluate the potency of purified MIC-1 as an anticancer compound. To accomplish this, we conducted a preliminary screen using 9 cancer cell lines and one non-tumorigenic cell line (Table 2). Cells were allowed to grow overnight before treatment with different concentrations of MIC-1, ranging from 200 nM to 1000 nM. Cells were allowed to incubate for 72 hours before cell viability was measured. As shown in Figure 4, the cancer cells were sensitive to MIC-1 with cell death observed in as little as 1µM of MIC-1. Interestingly, we observed hypersensitivity to MIC-1 in breast cancer cells overexpressing HER2. In addition, MCF10A, which is a non-tumorigenic breast cell line, was resistant to MIC-1. However, we factored in the fact that this is the only cell line grown on a different media enriched with growth hormones. Overall the breast cancer cell lines used in this were sensitive to MIC-1 treatment (figure 4a). Our results show MIC-1 is a potent anti-cancer compound.

A.
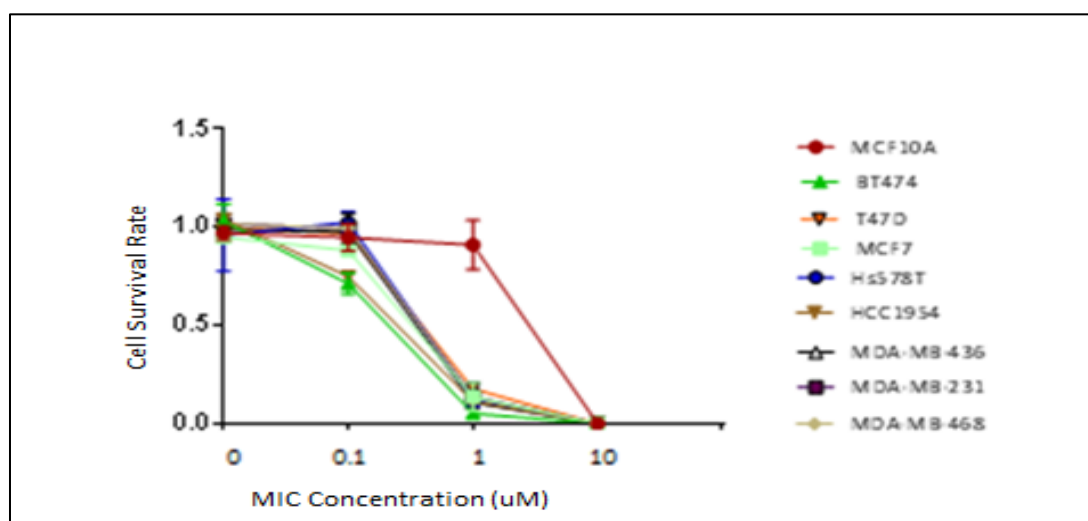
Figure 4a. Moringa Isothiocyanate a Potent Anticancer compound.
Cell Viability Assay showing breast cancer sensitivity to MIC-1. Assay shows a dose-dependent breast cancer cells sensitivity to MIC-1 after 72-hour incubation.

1.3.2 MIC-1 Is More Potent Than PEITC In Its Anti-cancer Activities

To better appreciate the efficacy of MIC-1 as an anticancer agent, we decided to examine the effect of a well-studied isothiocyanate, PEITC, on breast cancer cell lines compared to MIC-1. 9 breast cancer cell lines and one non-tumorigenic cell line were treated with different concentrations of PEITC (figure 4b). The breast cancer cells were more resistant to PEITC compared to MIC-1. While cell growth inhibition was observed with MIC-1 at about 1 uM concentration, for PEITC that did not occur until about 10 uM suggesting that MIC-1 was a more potent anti-cancer agent than PEITC. Here we show that 98% pure MIC-1 efficiently kills breast cancer cells in concentrations lower than those reported for other isothiocyanates studied and reported so far. The efficacy of this compound cuts across different types of breast cancer cells. The average IC50 value observed in the different cancer cells is 0.4. Comparing the potency of MIC-1 to well-studied

isothiocyanate PEITC, our studies show MIC-1 is more potent than PEITC. The average PEITC IC50 values observed across the same 9 breast cancer cell lines is 4 which is about 10 fold higher than MIC-1. Furthermore, our preliminary results suggest that overexpression of HER2 may play a role in hypersensitivity to MIC-1.

B.
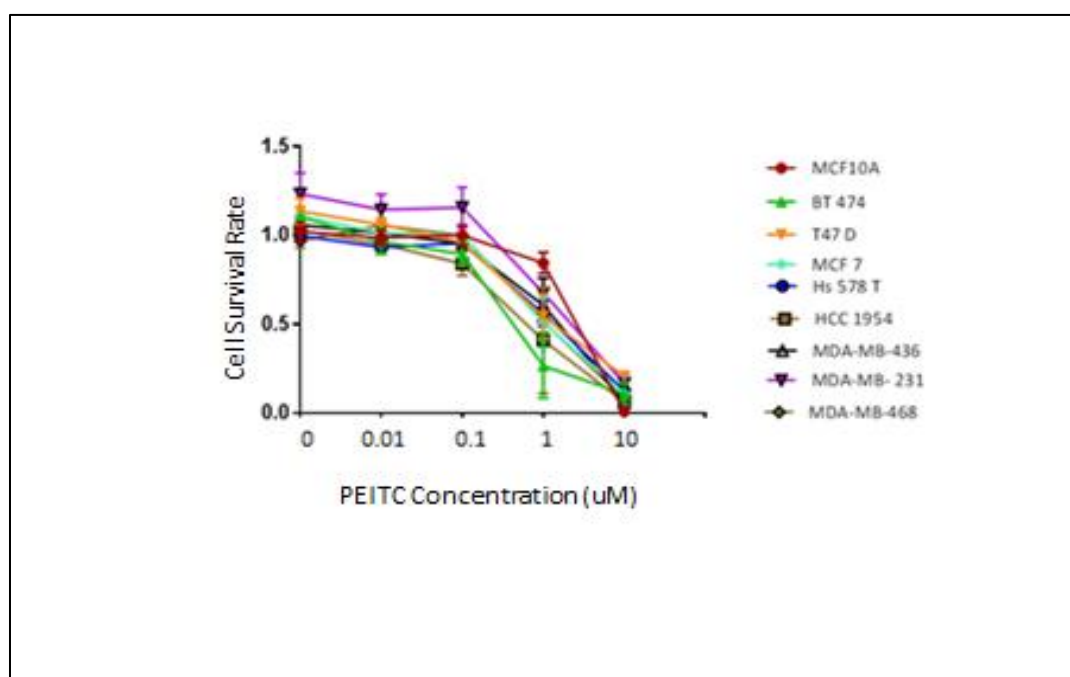
Figure 4b. Cell Viability Assay showing breast cancer sensitivity to PEITC.
A. Cell viability assay showing dose-dependent breast cancer cells sensitivity to PEITC after 72-hour incubation.

CHAPTER 2

HER2 Overexpression Induces Sensitivity In Breast Cancer Cells

<u>Summary</u>

Breast and ovarian cancer accounts for a third of cancers found in women. It is also responsible for a quarter of the cancer-related death in women. Studies by Slamon and colleagues 1987 showed that out of 189 primary human breast cancers examined 28% were found to have amplification of HER-2 (59). HER2 overexpression has been shown to be an indicator of poor prognosis (70).

Here we report that HER2 overexpression induces hypersensitivity to MIC-1. After our preliminary studies suggested HER2 overexpression may play a role in MIC sensitivity, we further confirmed this in follow up studies using MDA-MB-231 and MCF-7 both overexpressing HER2 along with their respective control.

2.1 HER2 Gene And Breast Cancer

HER2, a protein which is part of the epidermal growth factor receptor which has been observed to be amplified in a number of cancers. HER2 is reported to be overexpressed in 30% of breast cancer patients (70, 43, 65, 22)

HER2, also known as ERBB2 was originally identified in studies where NIH 3T3 cells were transformed with neuroglioblastomas originated DNA (69). HER2 belongs to the EGFR family of proteins, which has four members known as: HER1 (erbB1) HER2 (erbB2), HER3 (erbB3) and HER4 (erbB4) (42). Unlike other HER receptor proteins, which require ligand binding to be activated, HER2 protein is constitutively active (25, 12). HER2 signaling function is engaged by its heterodimeric partners once ligand bound as HER2 lacks ligand binding activity (71). HER3 protein, which has been shown to be HER2 obligate partner by several studies, is catalytically inactive due to its lack of ATP binding in its catalytic domain (66).

A type 1 transmembrane growth factor receptor, HER2 responds to extracellular cues to activate intracellular signals. HER2 structure consist of 3 domains: the intracellular tyrosine kinase domain, the transmembrane domain and the extracellular ligand binding domain. While HER2 function is very simple in *C. elegans*, the function is more complex in Drosophila and its most complex function is found in mammalians (45, 54).

Ligands bind to the extracellular domain of HER proteins, when this occurs, a conformation change occurs in the extracellular domain (90). This change promotes dimerization and trans phosphorylation of the HER intracellular

domain. The phosphorylated tyrosine residue activates several second messenger pathways resulting in different biological effects (91, 92, 93 ,94).

HER-2 /neu, a tyrosine kinase receptor has been observed to have a direct role in cell proliferation (17) and also in the repair of DNA damage (8). HER2/neu amplification is known to be a reliable predictor of clinical outcomes better than other known prognosticators (70).

Trastuzumab (Herceptin) which is an antibody specific for HER2 is a popular therapeutic for HER2 breast cancer cells but problems persist. Some breast cancers are known to have a specific type of HER2 known as p95. This form of HER2 has been shown to cause resistance to trastuzumab, this is because p95 lacks the extracellular domain that trastuzumab needs to for efficient binding to HER2 (64).

Internalization and degradation of HER2 has been proposed as the mechanism of action of trastuzumab. This is accomplished by triggering the tyrosine kinase-ubiquitin ligase c-Cbl and recruiting c-Cbl to its docking site upon binding of trastuzumab to HER2. C-Cbl signals HER2 for degradation by ubiquitinating HER2 (120)

Doxorubicin is another cancer therapeutic used to treat early stages of breast cancer. Research shows that a significant number of patients on doxorubicin therapy face a risk of cardiotoxicity at doses used for regular treatment (16). While a combined therapy involving doxorubicin may be effective for HER2,

doxorubicin does not downregulate HER2 but effectively downregulates EGFR (33).

Our objective is to examine if HER2 overexpression induces hypersensitivity to MIC-1.

2.2 Materials and Methods

2.2.1 Cell culture

Human breast carcinoma cell lines ZR-75-1, MDA-MB-453 were generous gift from Dr. Michael Gatza lab. These HER2 over-expressing cells were added to our collection of HER2 overexpressing cells BT474 and HCC1954. The HER2 overexpressing cells were studied along with HER2 negative cells MCF-7, MDA-MB-231. All cells used in this study were maintained in Gibco™ Dulbecco's Modified Eagle Medium: Nutrient Mixture F-12 (DMEM-F12) which was supplemented with 10% fetal bovine serum (FBS) and 1% penicillin. MCF7-FIR (MCF7 that overexpresses HER2 after repeated rounds of IR exposure) breast cancer cells used in this study was a generous gift from Dr. Jian Jian Li. The cells were generated after repeated passage of MCF7 cells and repeated exposure to radiation. MDA-MB-231-BR-HH (a brain-seeking HER2 overexpressing breast cancer cell line) was a generous gift from Dr. Patricia Steeg's lab, these brain seeking MDA-MB-231 cells were transfected with HER2.

2.2.2 Western Blot

In a time-dependent study, MCf7, MCF7-FIR, MDA-MB-231-BR-HH, and MDA-MB-231-BR- Vector 1μM of MIC-1 and allowed to grow at 30° for 1, 3 and 6 hours respectively. An extra plate without any treatment was prepared for each cell line as a control. Cells were trypsinized, cell pellets collected and sonicated in NET250 buffer. Both treated and untreated protein was subjected to gel electrophoresis. Gradient gel used in this study was prepared using 10%TEMED,

10% APS, 2M Tris (pH 8.8), 30% Bis-Acryl making 3% and 12% gradient gel. Separated protein was transferred to nitrocellulose membranes (Bio-rad cat# 1620115).

Primary antibody HER2 (Origene, Ratio of 1:5000 used) along with secondary antibodies (anti- mouse antibody) was used to develop the membrane and examine HER2 expression in the cells.

2.2.3 HER2 Knockdown using siRNA

HER2 (also known as ERBB2) was knocked down in HER2 overexpressing cells using different siRNA. The sense strands of the siRNAs are below:

ERBB2-419   GCCAGGUGGUGCAGGGAAA
ERBB2-876   GGGAGAGAGUUCUGAGGAU
ERBB2-1298   GCAUGGAGCACUUGCGAGA
ERBB2-1477   AUCACAGGUUACCUAUACA

Knock down incubation time was 48 hours.

2.2.4 ROS Measurement

To examine the effect of MIC-1 on ROS induction in breast cancer cells, approximately 1×10^6 cells were plated in 6 cm plates and allowed to grow up to 80% confluency. The cells were then treated with 1μM MIC-1 and allowed to incubate at different time points. Treatment with MIC was followed by incubation with 2, 7 dichlorofluorescin diacetate (DCFDA, 10 uM) for 30 minutes at 30 degrees.

Difference in intensity of DCFDA fluorescence among the different treatment groups for each cell line was measured using flow cytometry.

2.3 Results and Discussion

2.3.1 HER2 Positive cells are more sensitive to MIC.

To further investigate the role of HER2 overexpression in hypersensitivity to MIC, we expanded our collection of HER2+ breast cancer cells by adding ZR-75-1, and MDA-MB-453 to our collection. We observed that these new cell lines were more sensitive to MIC as well compare to HER2- counterparts (Figure 5a). We were curious to know how different HER2+ and HER2- cells were in basal ROS and GSH levels. In 2006, Trachootham and colleagues reported that inducing higher levels of ROS in epithelial ovarian cells led to increased sensitivity to PEITC. They transformed ovarian epithelial cells with Ras, which when activated led to higher intracellular ROS levels. The transformed epithelial cells and control were then treated with PEITC, their result showed that increased ROS levels in the oncogenically transformed cells induced hypersensitivity to PEITC. Studying another isothiocyanate, we wanted to investigate the basal ROS levels in HER2+ cells comparing them to HER2- cells. Our results show that all four HER2+ breast cancer cell lines had higher ROS levels than their HER2- counterparts did (Figure 5c). These results suggest that high ROS may trigger hypersensitivity to MIC in HER2+ cells. As shown in figure 5a and 5c respectively, the most sensitive HER2+ cell line (BT474) also has the most intracellular ROS levels, further confirming that ROS may play a role in the increased sensitivity observed in HER2+ cells. We also evaluated GSH levels in the cells, GSH levels were lower in HER2+ cell lines as expected with the exception of BT474. The high GSH

levels in BT474 may have been triggered in response to very high basal ROS

levels in the cell.
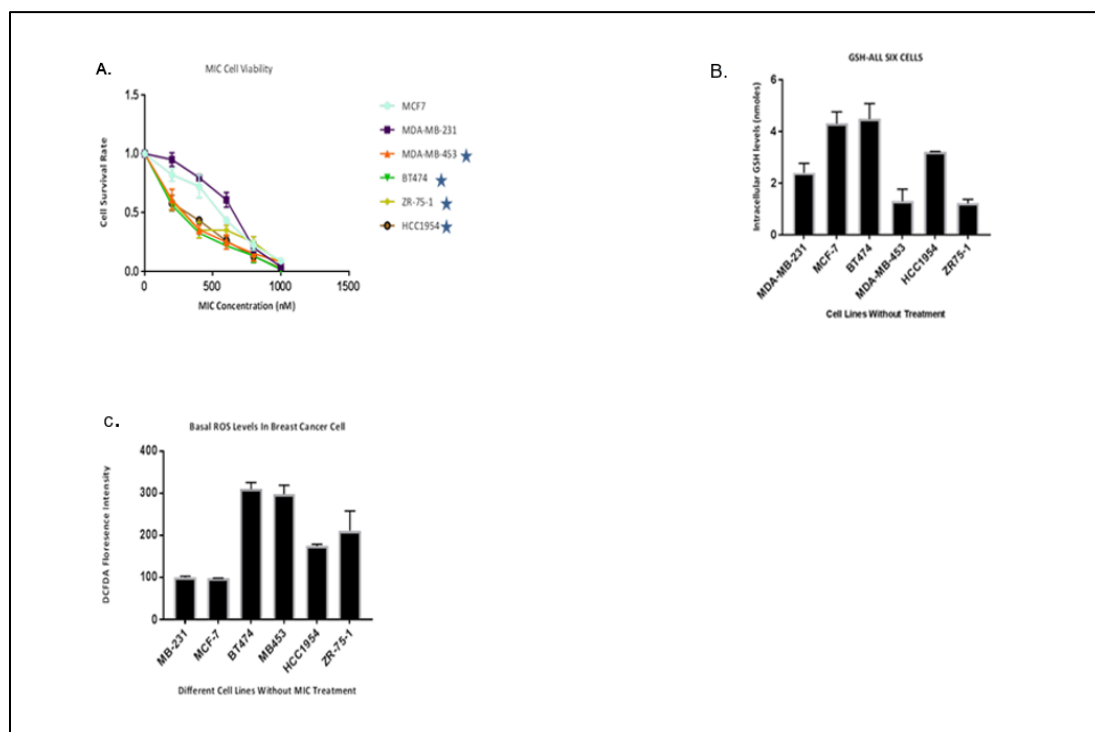
Figure 5. HER2 Overexpression induces hypersensitivity to MIC- I
  A. Cell viability assay showing a 4 HER2+ (★) with increased sensitivity to MIC in comparison to HER2- breast cancer cells
  B. Bar chart showing basal intracellular ROS in HER2- cells (MDA-MB-231 and MCF7) and HER2+ cells (BT474, MDA-MB-453, HCC1954, ZR-75-1)
  C. Bar chart showing basal intracellular GSH levels in both HER2- and HER2+ breast cancer cell lines

2.3.2 HER2 overexpression induces hypersensitivity to MIC-1 in transformed MDA-MB-231 and MCF-7 cells

To further establish the role of HER2 in MIC-1 sensitivity, MDA-MB-231-BR-HER2+ (overexpressing HER2) and MDA-MB-231-BR-vector (vector control) were treated with different doses of MIC and allowed to incubate for 72 hours. Cell viability was measured using cell titer Glo, measuring ATP levels in the 96 well plates. MDA-MB-231-BR-HER2+ showed significantly higher sensitivity to MIC compared to MDA-MB-231-BR-vector (Figure 6a). A similar result was observed when the study was repeated with MCF7-FIR and MCF-7 parental, MCF7-FIR was more sensitive to MIC-1 than MCF7 (Figure 6b). Western blot analysis of MCF7-FIR shows overexpression of HER2 in MCF7-FIR (4b) and overexpression of HER2 in MDA-MB-231 while the controls did not express HER2.

Data from our studies show that MIC-1 treatment considerably inhibits growth of HER2+ breast cancer cells at concentrations lower than that of their HER2-counterparts. MIC-1 also upregulates expression of HER2 in MCF7-FIR cell lines after treatment with MIC for 6 hours.

The effect of MIC-1 of the expression of NRF2 and KEAP1 was evaluated in MDA-MB-231-BR-HER2 along with MDA-MB-231-BR-vector control and MCF7-Fir. In MCF-7-Fir, we observed an upregulation of NRF2 in response to treatment with 1 μM of MIC-1 at 1 and 3-hour incubation time (figure 6d). The same response to treatment in terms of NRF2 expression levels was not observed in MDA-MB-231 (figure 6c).
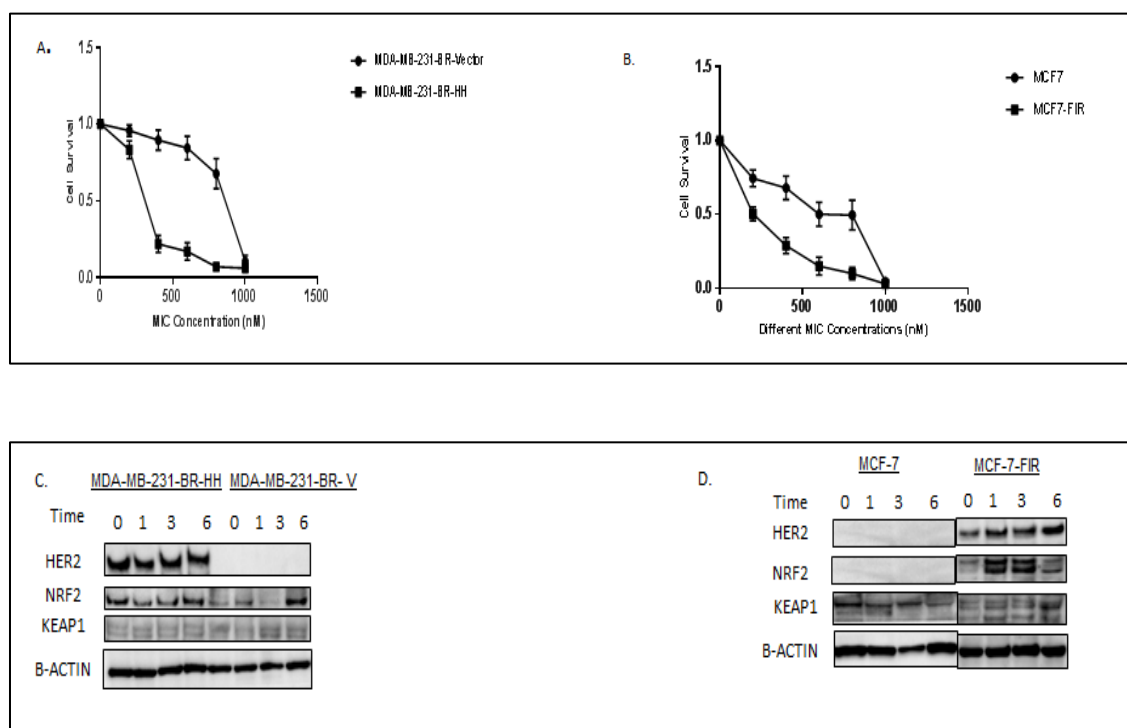
Figure 6: HER2 overexpression induces sensitivity to MIC -I:

A. Graph showing the response of HER2+ MDA-MB-231-BR-HH to MIC-1 in comparison to vector controls MDA-MB-231-BR-V
B. Graph showing the response of HER2+ MCF7-FIR to MIC-1 in comparison to control MCF7
C. Western blot analysis of HER2, NRF2, KEAP1 in MDA-MB-231-BR and MDA-MB-231-Vector after 1 μM MIC-1 treatment and incubation for 1,3 and 6 hours respectively.
D. Western blot analysis of HER2, NRF2, KEAP1 in MCF-7-FIR and MCF7-wildtype after 1 μM MIC-1 treatment and incubation for 1,3 and 6 hours respectively.

2.3.3 Effect of MIC-1 on ROS and GSH levels in HER2+ cells

As observed throughout the course of this study, the effect of MIC on intracellular ROS and GSH levels vary across the different cell lines. While MIC-1 triggered a sharp increase in ROS levels in some of the cells, no effect was observed in others. Here, while a drop was observed in ROS levels in MDA-MB-231-HH-BR after an hour treatment with 1 μM MIC no difference was observed in GSH levels at the same time point. The vector control for MDA-MB-231 however did not show any

changes in ROS level in response to MIC-1 treatment, this may be due to the increase observed in GSH levels after treating with ROS (Figure 7a and 7c). MCF7 Fir and MCF 7 both showed reduction in ROS levels in response MIC-1 treatment, while GSH levels in MCF7 did not change there was a sharp increase in GSH levels at the 6-hour time point for MCF7 Fir. While this data does not explain why HER2 overexpressing cells were more sensitive to MIC than their HER2 – counterparts, but it does show that MIC-1 adopts different mechanism in different   cell   lines.
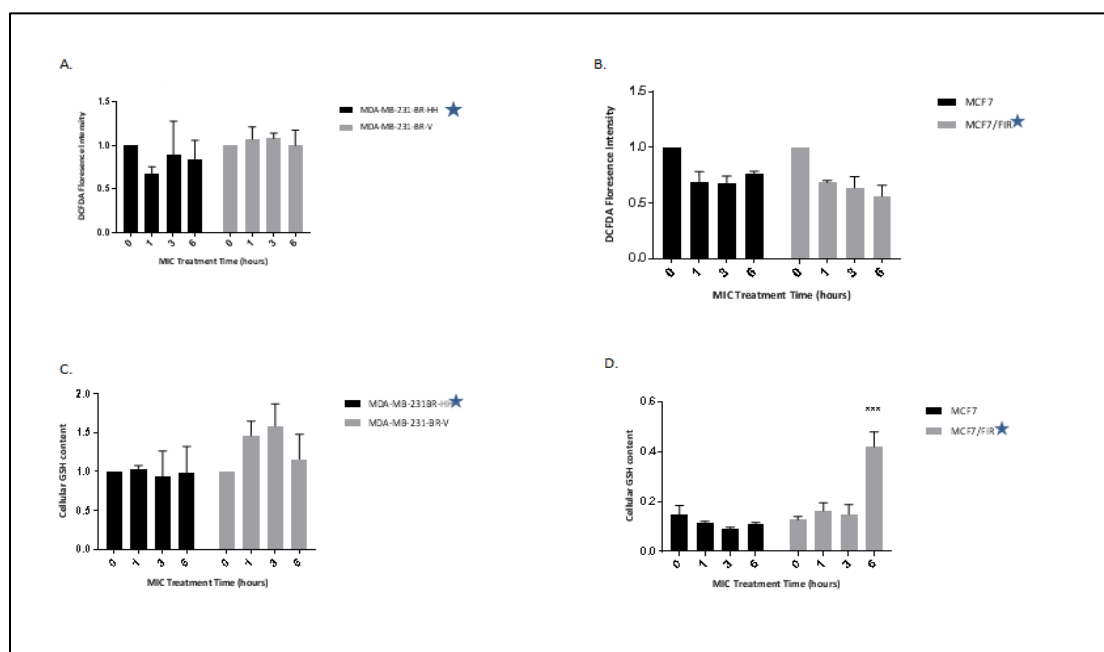
Figure 7. Effect of MIC-1 on ROS and GSH levels in MDA-MB-231-BR-HH and MCF7-FIR cells

A. Data showing the effect of 1 μM MIC-1 on intracellular ROS levels in MDA-MB-231-BR-HH and MDA-MB231-vector after 1, 3 and 6-hour incubation with MIC with 0 with 0 as no treatment control as control.
B. Data showing the effect of 1 μM MIC on intracellular ROS levels in MCF7-FIR and MCF7 after 1, 3 and 6-hour incubation with MIC-1.
C. Data showing the effect of 1μM MIC-1 on intracellular GSH levels in MDA-MB-231-BR-HH and MDA-MB231-vector after 1, 3 and 6-hour incubation with MIC.

D. Data showing the effect of 1µM MIC-1 on intracellular GSH levels in MDA-MB-231-BR-HH and MDA-MB231-vector after 1 ,3 and 6-hour incubation with MIC

2.3.4 HER2 Knockdown Reduces HER2+ Cancer Cell Proliferation

To examine the role of HER2 overexpression in inducing higher sensitivity to MIC-1, we knocked down HER2 in BT474 (Figure 8). Our objective was to observe if resistance to MIC will be observed in this HER2 overexpressing cells after HER2 knockdown. This was also repeated for MDA-MB-453 and HCC1954 (figure 9). We examined the effect of this HER2+ knock down on sensitivity to MIC-1 and on cell proliferation as well.
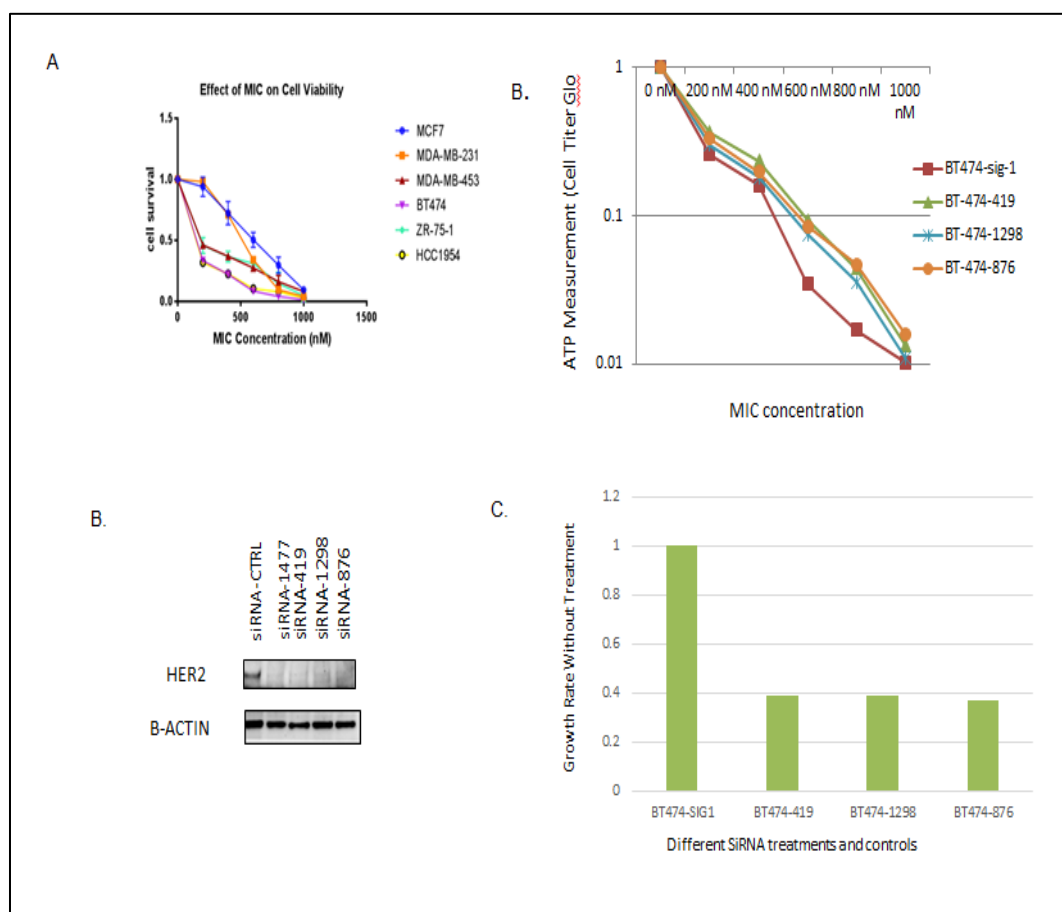
Figure 8: HER2 knockdown inhibits breast cancer cell proliferation:

A. Graph showing the response of HER2+ cells (BT474, ZR-75-1, MDA-MB-453) to MIC-1 in comparison to HER2- breast cancer cells (MCF7 and MDA-MB-231)
B. Cell viability assay results showing the response of BT474 cells with knocked down HER2 to MIC-1 compare to control BT474 cells (SiRNA-Ctrl)
C. Western blot analysis of HER2 showing the efficacy of HER2 knockdown in BT474 using different HER2 siRNAs
D. Chart showing the effect of HER2 knockdown on cell proliferation.
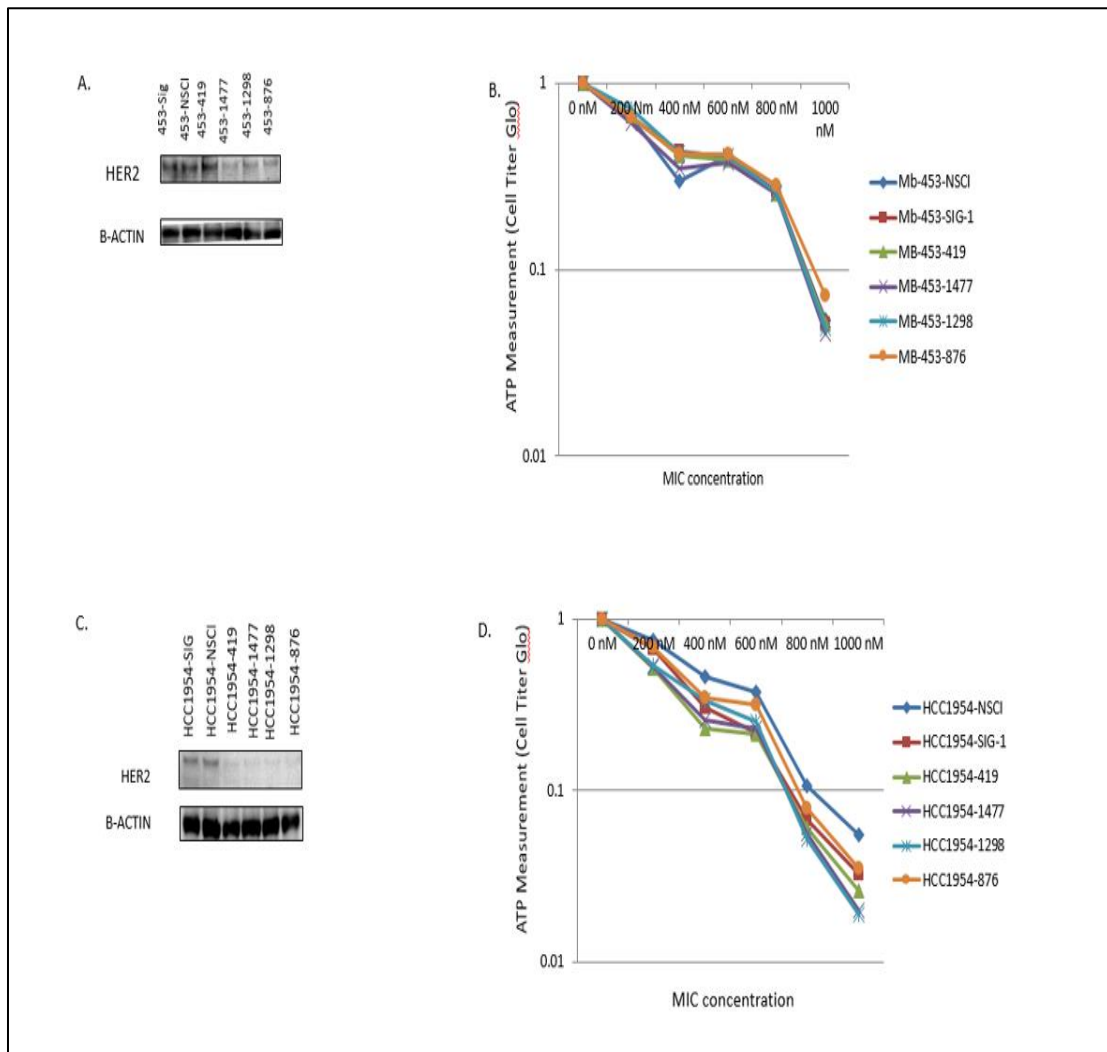
Figure 9: Effect of HER2 knockdown on resistance/sensitivity to MIC-1

A. Western blot analysis of HER2 showing the efficacy of HER2 knockdown in MDA-MB-453 using different HER2 siRNAs along with control siRNA (SIG and NSCI)

B. Cell viability assay results showing the response of MDA-MB-453 cells with knocked down HER2 to MIC-1 compare to control MDA-MB-453 cells (SiRNA- Sig and NSCI which are controls)

C. Western blot analysis of HER2 showing the efficacy of HER2 knockdown in HCC 1954 using different HER2 siRNAs along with control siRNA (SIG and NSCI)

D. Cell viability assay results showing the response of HCC1954 cells with knocked down HER2 to MIC-1 compare to control HCC1954 (SiRNA- Sig and NSCI which are controls)

While resistance to MIC-1 was observed in BT474 after an efficient HER2 knock-down we did not observe a similar observation in MDA-MB453 (figure 9b) and HCC1954 (figure 9d). However, we noticed that HER2 knock down inhibits proper proliferation of HER2+ cells as shown for BT474 (Figure 8d). This further confirms that HER2 is essential for growth of HER+ cells as previously reported by Lee-Hoeflich and colleagues in 2008. In their work, Lee-Hoeflich and colleagues showed that knocking down HER2 in different HER2 + cell lines reduced cell proliferation in these cells.

CHAPTER 3

MIC-1 Regulates NRF2 KEAP1 In Breast Cancer Cells

Summary

Reactive oxygen species (ROS) are generated from both intragenous and extraneous sources in eukaryotic cells. ROS consist of a group of radical and non-radical species that are oxygen derived. These radical species include superoxide, hydroxyl and peroxyl while the non-radical species include hypoclorus acid, hydrogen peroxide and singlet oxygen (37, 30). Cellular oxidative stress results when there is a loss in homeostasis in ROS production and elimination in the cell. Key regulators of intracellular ROS levels are NRF2 and the KEAP1, which play important role in regulation of phase 2 enzymes.

Here we show that MIC regulates ROS levels in some breast cancer cell lines and also regulates NRF2 and KEAP1 in a cell line dependent manner.

3.1. NRF2 –KEAP1 Pathway

3.1.1 NRF2

The NRF2-KEAP1 pathway is an important pathway in the regulation of oxidative stress caused by electrophiles and reactive oxygen species (38).

Nuclear Erythroid Factor 2 (Nrf2) is a bZIP transcription factor, with six evolutionary conserved domains Neh 1-6.
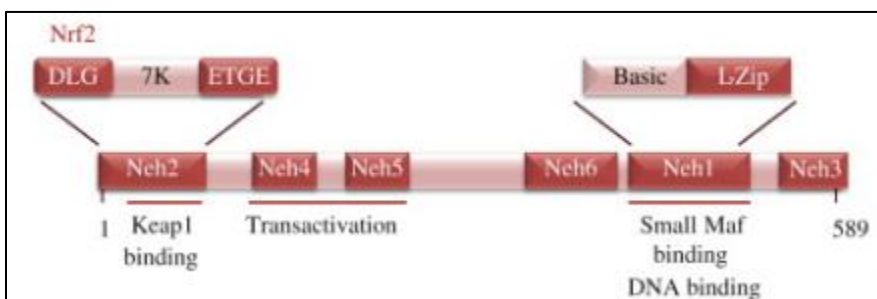
Figure 10 : NRF2 Structure showing conserved domains Neh 1, a leucine zipper structure which plays a role in DNA recognition and dimerization with small Maf proteins, Neh 2 which contain DLG and ETGE motifs which are important for interaction with KEAP1 along with Neh 3, 4,5 and 6. Image adapted from Kansanen et al 2013, Redox Biology

NRF2 that binds to the antioxidant response elements (ARE) along with MAF is a key signaling protein. The binding of NRF2 and MAF to ARE triggers the expression of targeted antioxidant genes (38).

One of the NRF2 domains that serves as a platform for ARE binding is Neh1 domain, it contains a basic leucine zipper motif. Neh2 domain and the Neh 3 domain are located on opposite sides of the each other, while Neh2 is on the N-terminal region, Neh 3 domain is located in the C-terminal region. These regions are important as the Neh2 domain functions as a negative regulatory domain and the Neh 3 domain functions as the NRF2 transactivator. Neh 4 and Neh 5 appear to play a support role in Neh3 activity and are essential for NRF2 transactivation (40, 74).

Under normal conditions, NRF2 is located in the cytoplasm and is kept at low levels due to consistent ubiquitination and subsequent degradation. However, when oxidative stress is high in the cell, NRF2 is significantly induced and migrates into the nucleus where it binds to ARE along with MAF to trigger the activation of cytoprotective enzymes such as NADPH: quinone oxidoreductase-1 (NQO1), glutathione S-transferase (GST), γ-glutamylcysteine ligase and heme oxygenase 1 (95).

A cysteine rich repressor protein called Kelch ECH associating protein 1 (KEAP1) regulates NRF2. KEAP1 binds to NRF2 and promotes its ubiquitination (74).
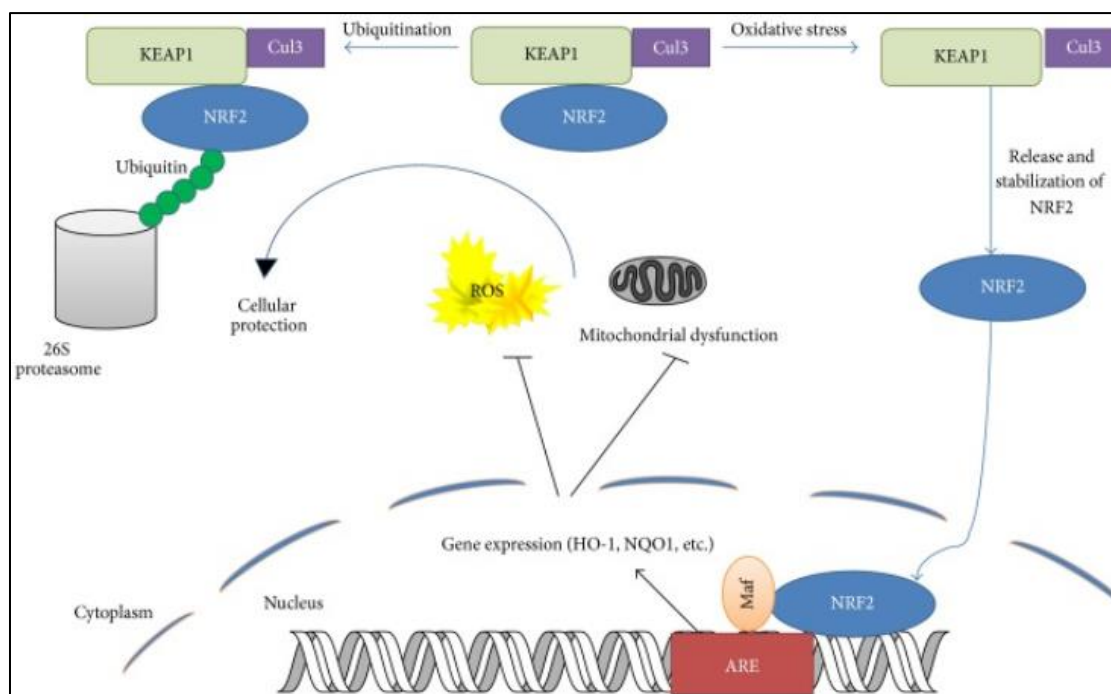
Figure 11. NRF2- KEAP1 Interaction. Illustration showing the NRF2 – KEAP1 interaction and the process of ubiquitination of NRF2 as well as its activities in the nucleus. Image culled from Kim and Keum 2011. Oxid Med Cell Longev. 2016; 2016: 2746457.

3.1.2 KEAP1

KEAP1 binds to NRF2 via its Neh2 domain , and as previously described, signals

NRF2 for ubiquitination. KEAP1 has been shown to act as a Cullin-3-based E3's

adaptor; together they inhibit NRF2 activity (48). KEAP1, a cysteine rich protein,

has been shown to have several cysteine residues, specifically 25 and 27 cysteine

residues in mouse and human respectively (38). KEAP1 is also known to have two

domains that interact with proteins, the BTB (bric-a-brac, tramtrack, broad-

complex) domain found in the N-terminal while the Kelch repeats are found in

the C terminal. BTB mediates the binding of Cul3 to KEAP1 while the Kelch

repeat region mediates the NRF2 –KEAP1 binding. Located between the N and C

terminals of KEAP1 is the intervening region (IVR) which is also known as the

linker region (LR) (55, 48, 56). Mutation in KEAP1 residues could affect the

binding of NRF2 to KEAP1 and subsequently the ROS levels in the cell are

elevated. C151, C273, C288 are residues whose modifications have been shown to

lead to functional changes in KEAP1. These conformational changes in KEAP1

prevents NRF2 binding to KEAP1, hence levels of NRF2 in the cytoplasm

increases leading to NRF2 migration to the nucleus for ARE binding/target gene

expression (74)
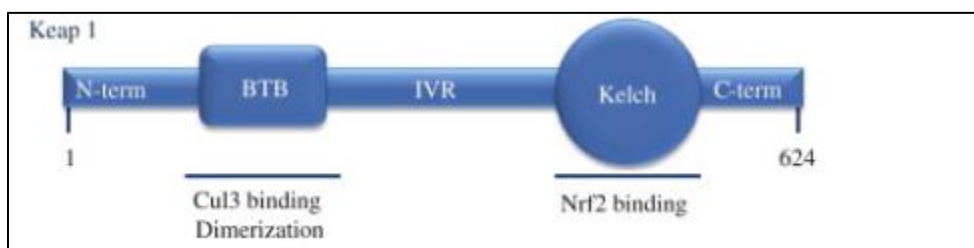
Figure 12: Keap1 Structure Showing 5 domains. Image showing the
Kelch domain, BTB domain and the intervening region which separates the

Kelch domain and the BTB domain. Image adapted from Kansanen et al 2013, Redox Biology, Volume 1, Issue 1, 2013, 45–49

The half-life of NRF2 has been reported to be approximately 20 minutes. KEAP1 brings NRF2 to the E3 complex where NRF2 binds to CUL3N terminal through KEAP1's DGR domain (32, 44, 48). Results from a nuclear magnetic resonance titration study by Tong and colleagues (75) clarified the mechanism of KEAP1 regulation of NRF2 ubiquitination.
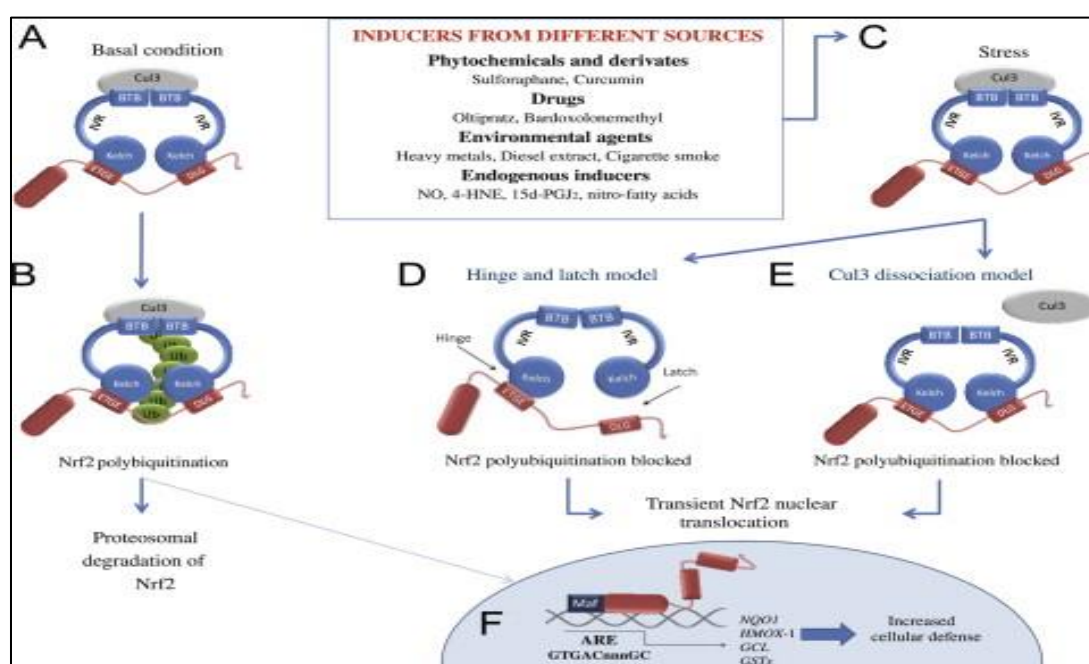
Figure 13 : Model for NRF2-KEAP1 interaction (A and B) show the KEAP1 and NRF2 interaction under basal condition. (C) show that inducers modify KEAP1 preventing proper binding of NRF2, leading to inhibition of NRF2 ubiquitination (D and E) Shows models explaining the possible changes that occur in KEAP1, disrupting proper NRF2 binding and NRF2 polyubiquitination. (Picture adapted from Kanasen et al. 2013).

3.1.3 NRF2/SMALL MAF Heterodimer /ARE and Phase II Detoxifying enzyme induction

NRF2 is known to activate the induction of phase II detoxifying enzymes by forming heterodimers with small MAF (sMAF) protein and then binding to antioxidant response element (ARE) thereby regulating the intracellular ROS levels (34).

Xenobiotics from extracellular environment has been shown to trigger the activities of detoxifying enzymes (59). The detoxifying enzymes convert these xenobiotics into less toxic substances that can readily dissolve in water. The process starts with the activities of phase 1 enzyme cytochrome P-450 mono-oxygenase which is then followed by phase 2 reactions catalyzed by quinone oxidoreductase (NQO1), gluthathione S-transferases (GST) and NADPH (11).

3.1.4 Gluthathione

Gluthathione is abundant in the cells and is probably the most abundant thiol and low molecular weight peptide in the cell. Gluthathione is involved in detoxifying xenobiotics in the cell, also functions as a reducing agent as well as an antioxidant (41).

Also, gluthathione plays a role in the metabolism of several compounds within the cell. It has also been shown to be involved in prostanglandins synthesis. Cell cycle regulation and thermotolerance are cellular activities that have been attributed to gluthathione (10, 23, 53, 58, 60, 67, 82). Protecting the cells against damage from hyperoxia, UV damage and phytodyanmic effect are some of the roles reported for gluthathione (14, 28,29, 13, 52)

The synthesis of gluthathione which utilizes ATP and is catalyzed by the enzyme λ-glutamylcysteine synthase is a two-step reaction. The first step in this reaction is the rate limiting step and can be inhibited by GSH in a feedback regulation loop. Substrates for the synthesis of gluthathione are amino acids (2, 51, 61).

Oxidized gluthathione (GSSG) is produced in the cell through the gluthathione reductase reaction, accumulation of GSSG signals depletion of GSH. A series of intracellular reactions regulate the GSH and GSSG levels. Under normal cellular homeostatic conditions, reduced GSH is preferred in the cell (4, 14, 19, 35,36)

3.2 Materials and Methods

3.2.1 Western Blot

In a time-dependent study, MCf7, MDA-MB-231, BT474, HCC1954, MDA-MB-453 and ZR-75-1 1μM of MIC-1 and allowed to grow at 30° for 1, 3 and 6 hours respectively. An extra plate without any treatment was prepared for each cell line as a control. Cells were trypsinized, cell pellets collected and sonicated in NET250 buffer. Both treated and untreated protein were subjected to gel electrophoresis. Gradient gel used in this study was prepared using 10% TEMED, 10% APS, 2M Tris (pH 8.8), 30% Bis-Acryl making 3% and 12% gradient gel. Separated protein was transferred to nitrocellulose membranes (Bio-rad cat# 1620115).

Primary antibodies for NRF2 (Abcam, Cambridge, MA. Ratio of 1:2000 used), Keap1 (Santa Cruz, CA. Ratio of 1:5000 used), HER2 (Origene, Ratio of 1:5000 used). Secondary antibodies specific for each of the above listed primary antibodies were used to develop the membrane.

3.2.2 Gluthathione (GSH) assay: Glutathione assay kit was purchased from Sigma Aldrich (Louis MO). Manufacturer's protocol was adhered to in collecting cell lysate from the breast cancer cells and measuring glutathione in the cells. MCf7, MDA-MB-231, BT474, HCC1954, MDA-MB-453 and ZR-75-1 breast cancer cells were treated with 1μM MIC-1 in a time dependent assay. The effect of MIC-1 on intracellular GSH levels was measured using GSH Assay Kit.

3.2.3 ROS Measurement

Intracellular ROS levels were measured in the HER2 positive and HER2 negative cells using dichlorofluorescin diacetate (DCFDA). Approximately 1×10^6 cells were plated in 6 cm plates and allowed to grow to 80% confluency. These breast cancer cells were treated with MIC-1 in a time dependent manner before treatment with DCFDA. Cells treated with DCFDA were allowed to incubate at 37 degrees for 30 minutes. Difference in intensity of fluorescence was measured using flow cytometry.

3.2.4 Quantitative-PCR

RNA was extracted from MDA-MB-231 and MDA-MB- 453 cell lines treated with 1μM MIC-1 for 1, 3, and 6 hours respectively. RNA extraction and purification was done using the RNeasy plus mini kit by Qiagen Company. RNA concentration was measured using nanodrop and RNA quality was evaluated using 1.5% agarose gel. Complementary DNA was synthesized using 1μg of RNA and superscript III first strand synthesis system for RT-PCR (Life Technologies). Primers for NRF2 (5' ATTCCCGTTTGTAGATGACAATC), KEAP1 (5" CAGTGGACAGGTTGAAGAACT). Primers (12.5μM), DEPC treated water and SYBR ROX (life technologies) was used to prepare a master mix. PCR was performed using 96 well plates measuring the expression of four genes. Real life Time Systems QPCR was used following the manufacturer's instructions.

3.2.5 Co-Immunoprecipitation

To detect the interaction of NRF2 and KEAP1 after MIC-1 treatment, immunoprecipitation (IP) and western blotting was done. MDA-MB-231 cells were plated in 6cm plates and allowed to grow for 48 hours. Cells were treated with 1µM MIC and allowed to incubate for 1, 3 and 6 hours respectively. One plate was not treated with MIC-1 at all to serve as a control. Cells were later trpsinized, harvested and lysed in 500 µl NETNG 250.

IP was carried out by adding 1 µl NRF2 rabbit monoclonal (ab62352, Abcam) and 5 µl of protein A beads (Roche), 350 µl of lysate. This was allowed to rock at 4 degrees overnight. Beads were washed three times with cold NETNG 250 before western blot analysis. Cell lysates were resolved on 3-12% polyacrylamide gel. The protein was transferred onto nitrocellulose membranes following electrophoresis. Blots were probed with primary antibody for 2 hours at room temperature followed by secondary antibody for 1 hour. Blots were later developed using Immobilon Western Chemiluminescent (Millipore). The primary antibodies used are: KEAP 1 polyclonal (Santa Cruz) NRF2 rabbit monoclonal (Abcam), secondary antibodies used are donkey anti-rabbit (GE Healthcare) and Bovine anti-goat IgG (Jackson Immunoresearch)

3.3 Results and Discussion

3.3.1 MIC Regulates ROS Levels in Breast Cancer Cells

Since MIC regulates the key regulators of oxidative stress, coupled with different studies reporting that certain isothiocyanates adopt an ROS mediated pathway, we decided to examine the effect of MIC-1 on intracellular ROS levels. Our preliminary study using 10 different cell lines measured intracellular ROS changes in response to MIC-1 after 30 minutes and 60 minutes' incubation with MIC-1 in a cell-type dependent manner. Our data shows MIC triggers about a 2-fold increase in ROS levels in Hs578T and T47D (Figure 14) after about 60 minutes' incubation with MIC-1, while a 5-fold increase in ROS was observed in MDA-MB 468 at about the same time point. Interestingly, a similar result was observed with the same cell lines after treatment with PEITC (figure 15), ROS was generated in Hs578T, T47D and MDA-MB-468. Work by Gupta and Srivastava, has previously shown that PEITC induces ROS generation in cells. This data goes on to suggest that similar to PEITC, MIC-1 may adopt ROS mediated pathway in some of the breast cancer cells. While MDA-MB-231 and BT474 showed a difference in intracellular ROS levels in response to MIC-1 treatment at different

time points others did not.
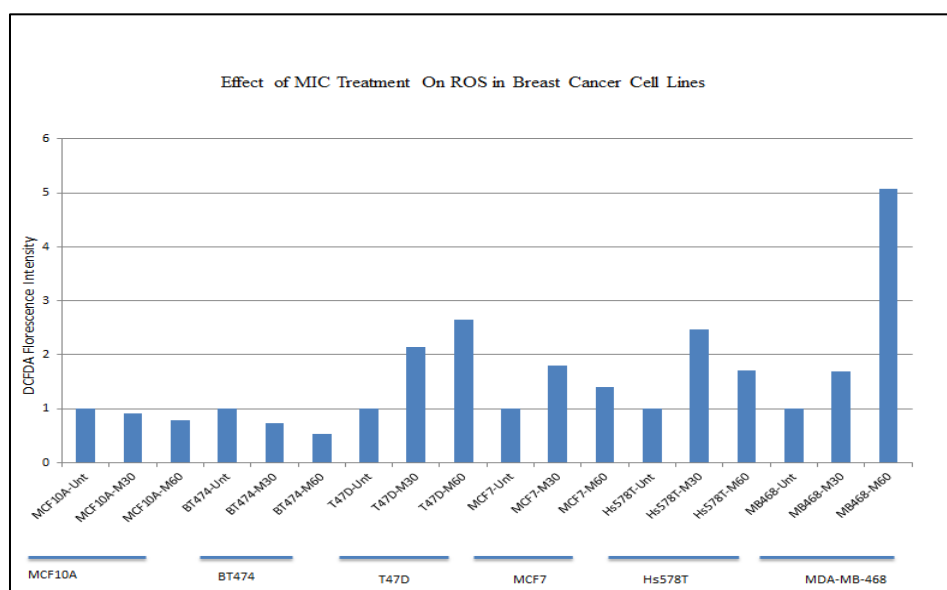
Figure 14: Effect of MIC-1 on Intracellular ROS Levels at 30 and 60 minutes
Chart showing the effect of 1 µM of MIC-1 on the ROS levels in MCF10A, BT474, T47D, MCF7, Hs578T and MDA-MB-468 after 30 minutes and 60 minutes incubation time
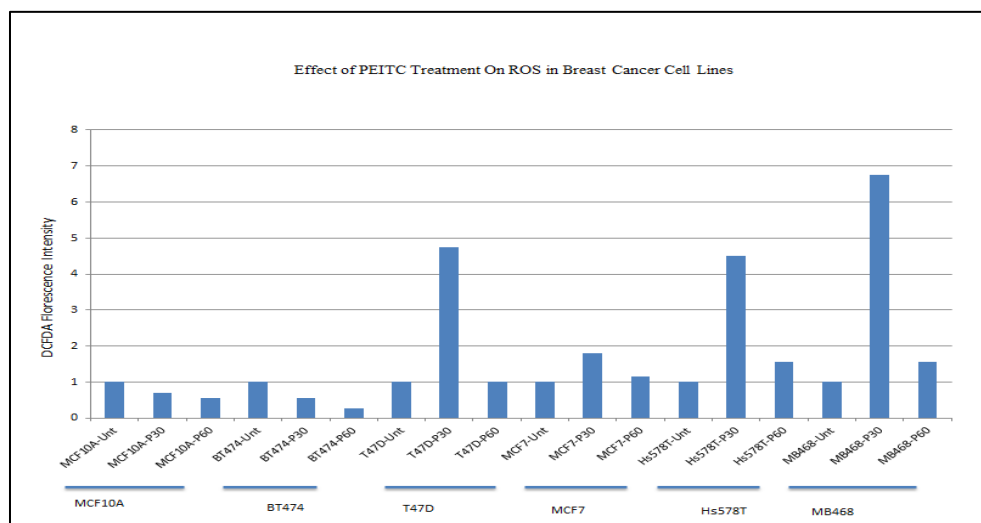
Figure 15: Effect of PEITC on Intracellular ROS Levels at 30 and 60 minutes
Chart showing the effect of 10 uM of PEITC on the ROS levels in MCF10A, BT474, T47D, MCF7, Hs578T and MDA-MB-468 after 30 minutes and 60 minutes incubation time.

Treating MDA-MB-231 with 1 μM of MIC-1 for 1, 3 and 6 hours respectively

showed a reduction in ROS levels within the first hour of treatment. The

reduction in ROS was maintained at the 3-hour time point but later elevated at

the 6-hour time point. Bt474 also showed a drastic change in ROS levels in

response to 1 μM MIC treatment. While these two cell lines, which are HER2- and

HER2+ respectively, respond to MIC-1 with changes in ROS levels, HCC1954,

MDA-MB-453, ZR75-1 and MCF 7 did not respond with ROS level changes. This

data suggest that the HER2 status of the cell line does not dictate ROS response

of the cell to MIC-1.

A.

B.

Figure 16: MIC-1 Regulates ROS Levels in Cells
  A. Histogram showing the effect of on ROS levels in ZR-75-1 and HCC1954
     after 1, 3 and 6 hours of treatment, with no treatment labeled 0
  B. Histogram showing the effect of on ROS levels BT474 and MDA-MB-453
     after 1, 3 , and 6 hours of treatment, with no treatment labeled 0

Figure 16c . Effect of MIC-1 on MDA_MB -231 ROS Levels. Histogram showing the effect of MIC on ROS levels MDA-MB-231 and MCF7 after 1, 3 , and 6 hours of treatment, with no treatment labeled 0

3.3.2 MIC Regulates NRF2 KEAP1 in Breast Cancer Cells

NRF2 −KEAP1 pathway plays an important role in managing intracellular ROS levels. We examined the effect of MIC-1 on breast cancer cells by treating cells with 1 μM MIC for different time points (1, 3, 6 hours respectively). We then evaluated the effect of MIC-1 treatment on the expression of NRF2, KEAP1 and their downstream targets. We observed that MIC-1 upregulates NRF2 in MDA-MB-453 and upregulates KEAP1 at the 6 hour time point in MDA-MB-453. Upregulation of NRF2 was also observed in MDA-MB-231 along with changes in intracellular ROS levels.

The reduction in intracellular ROS levels in MDA-MB -231 also corresponded with the upregulation observed in NRF2 protein expression at the same time point. At the one-hour time point, an increase in NRF2 protein expression levels (figure 16a) was observed and a decrease in ROS levels was observed as well

(figure 16b), this drop in ROS level was sustained at the 3 hour time point before an increase was observed at the 6 hour time point. This data suggests that the upregulation of NRF2 in this cell line may be a functional one with NRF2 doing its job of regulating ROS levels in the cell effectively. Treatment of MDA-MB-453 with 1 μM of MIC-1 for 1, 3 and 6 hours gave a completely different response with regards to intracellular ROS levels. There were no changes in ROS levels (figure 17b) observed in MDA-MB-453 even though changes upregulation of NRF2 (figure 17a) was observed in the cell line. This data suggests a non-functional upregulation of NRF2, which could be due to a disruption in NRF2 interaction with KEAP1. Interaction with KEAP in a way that prevent the ubiquitination of NRF2, hence NRF2 is not signaled for degradation. This hypothesis explains why we have co-upregulation of both NRF2 and KEAP1 in breast cancer cells. We also observed that in ZR-75-1, MIC-1 did not trigger any changes in NRF2 nor KEAP1 (figure 21a) neither was any changes in intracellular ROS levels observed in response to MIC-1 treatment (figure 21 c). This data suggest that MIC-1 mechanism of action will vary across different cell lines. In addition, it shows that the different mechanism adopted is not a function HER2 status.
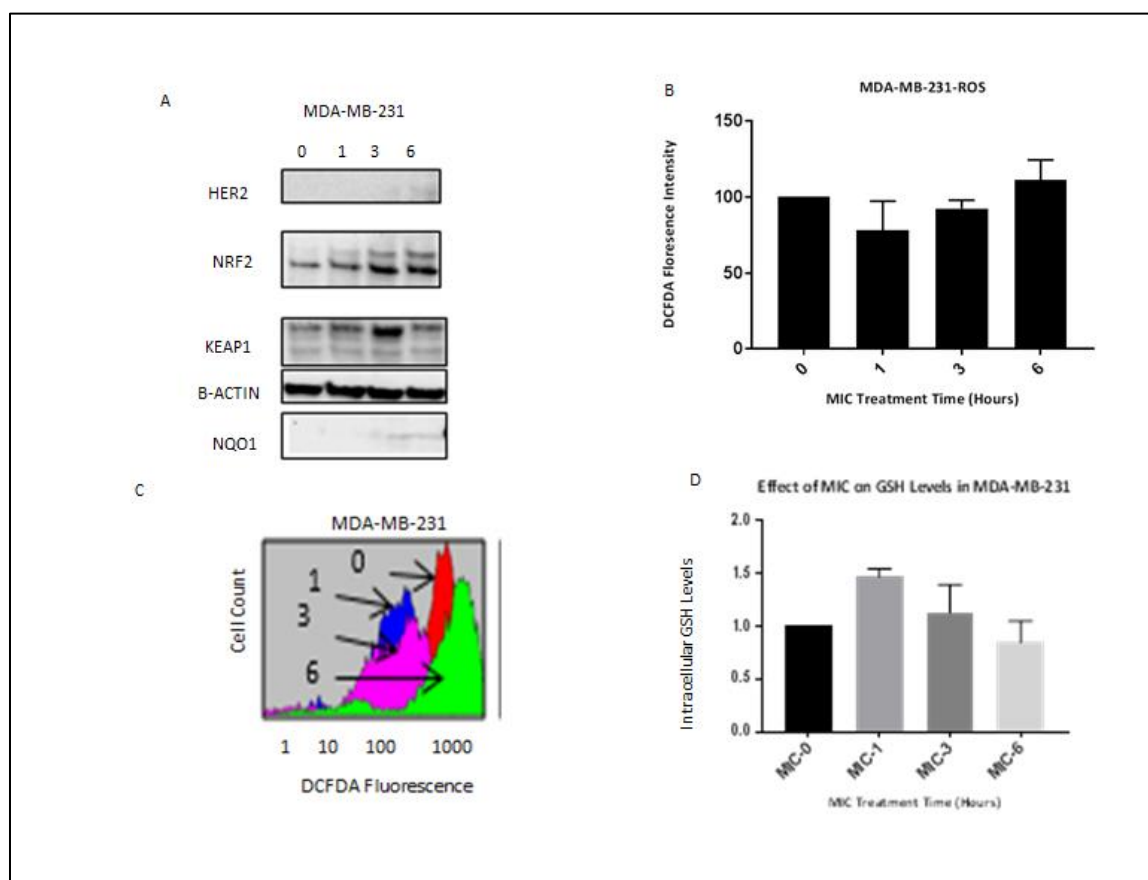
Figure 17: MIC-1 upregulates NRF2 in MDA-MB231
    A. Western Blot Analysis of HER2, NRF2, KEAP1, and NQO1 after treatment with 1 µM of MIC-1 and incubation for 1, 3, 6 hours with no MIC-1 treatment labeled as 0
    B. Chart showing changes in ROS levels in response to 1 µM MIC-1 treatment and incubation for 1, 3, 6 hours with no MIC-1 treatment labeled as 0
    C. Histogram showing changes in ROS levels in response to 1 µM MIC-1 treatment and incubation for 1, 3, 6 hours with no MIC-1 treatment labeled as 0
    D. Chart showing changes in GSH levels in response to 1 µM MIC-1 treatment and incubation for 1, 3, 6 hours with no MIC treatment labeled as 0

Figure 18: MIC upregulates NRF2 in MDA-MB453
  A. Western Blot Analysis of HER2, NRF2, KEAP1, and NQO1 after treatment with 1 μM of MIC and incubation for 1, 3, 6 hours with no MIC-1 treatment labeled as 0
  B. Chart showing changes in ROS levels in response to 1 μM MIC-1 treatment and incubation for 1, 3, 6 hours with no MIC-1 treatment labeled as 0
  C. Histogram showing changes in ROS levels in response to 1 μM MIC-1 treatment and incubation for 1, 3, 6 hours with no MIC-1 treatment labeled as 0
  D. Chart showing changes in GSH levels in response to 1 μM MIC-1 treatment and incubation for 1, 3, 6 hours with no MIC-1 treatment labeled as 0
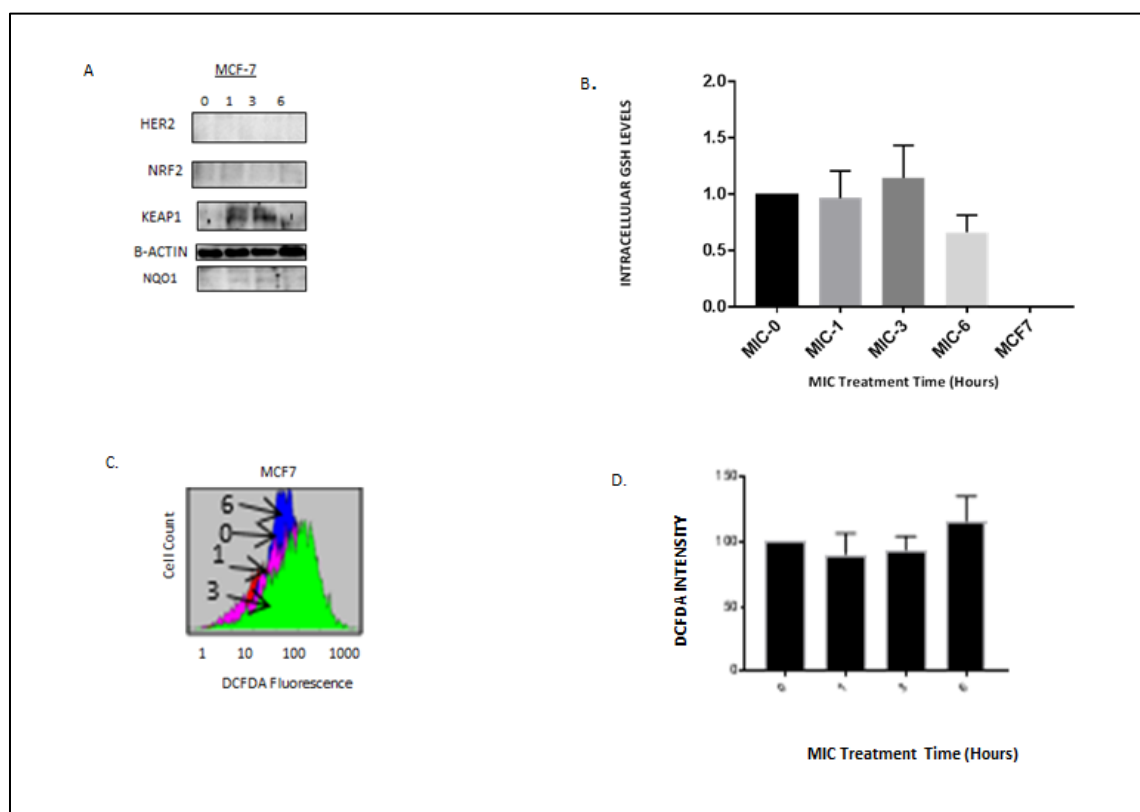
Figure 19: MIC-1 upregulates KEAP1 in MCF7

    A. Western Blot Analysis of HER2, NRF2, KEAP1, and NQO1 after treatment with 1 μM of MIC and incubation for 1, 3, 6 hours with no MIC-1 treatment labeled as 0

    B. Chart showing changes in ROS levels in response to 1 μM MIC-1 treatment and incubation for 1, 3, 6 hours with no MIC treatment labeled as 0

    C. Histogram showing changes in ROS levels in response to 1 μM MIC-1 treatment and incubation for 1, 3, 6 hours with no MIC-1 treatment labeled as 0

    D. Chart showing changes in GSH levels in response to 1 μM MIC-1 treatment and incubation for 1, 3, 6 hours with no MIC treatment labeled as 0
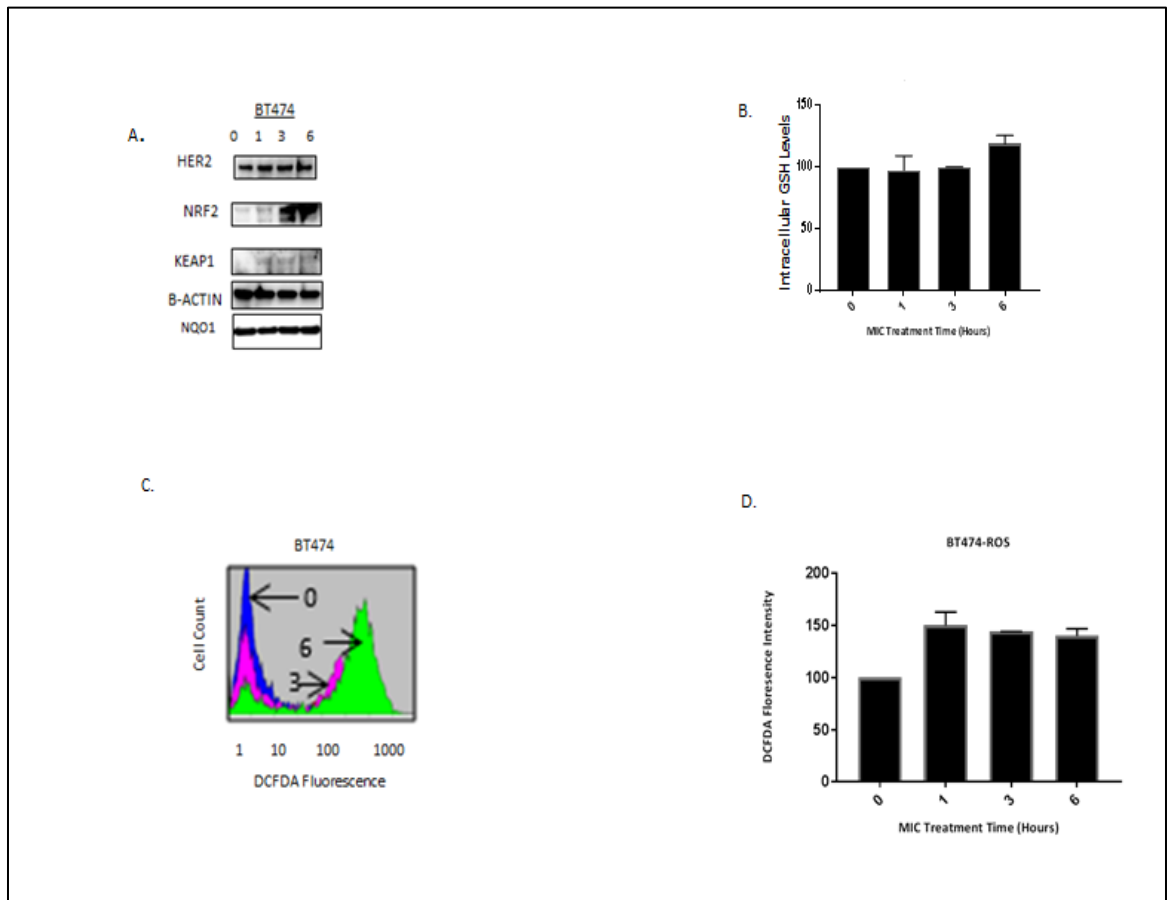
Figure 20: MIC-1 upregulates NRF2 in BT474
    A. Western Blot Analysis of HER2, NRF2, KEAP1, and NQO1 after treatment with 1 μM of MIC-1 and incubation for 1, 3, 6 hours with no MIC-1 treatment labeled as 0
    B. Chart showing changes in ROS levels in response to 1 μM MIC-1 treatment and incubation for 1, 3, 6 hours with no MIC treatment labeled as 0
    C. Histogram showing changes in ROS levels in response to 1 μM MIC-1 treatment and incubation for 1, 3, 6 hours with no MIC-1 treatment labeled as 0
    D. Chart showing changes in GSH levels in response to 1 μM MIC-1 treatment and incubation for 1, 3, 6 hours with no MIC treatment labeled as 0
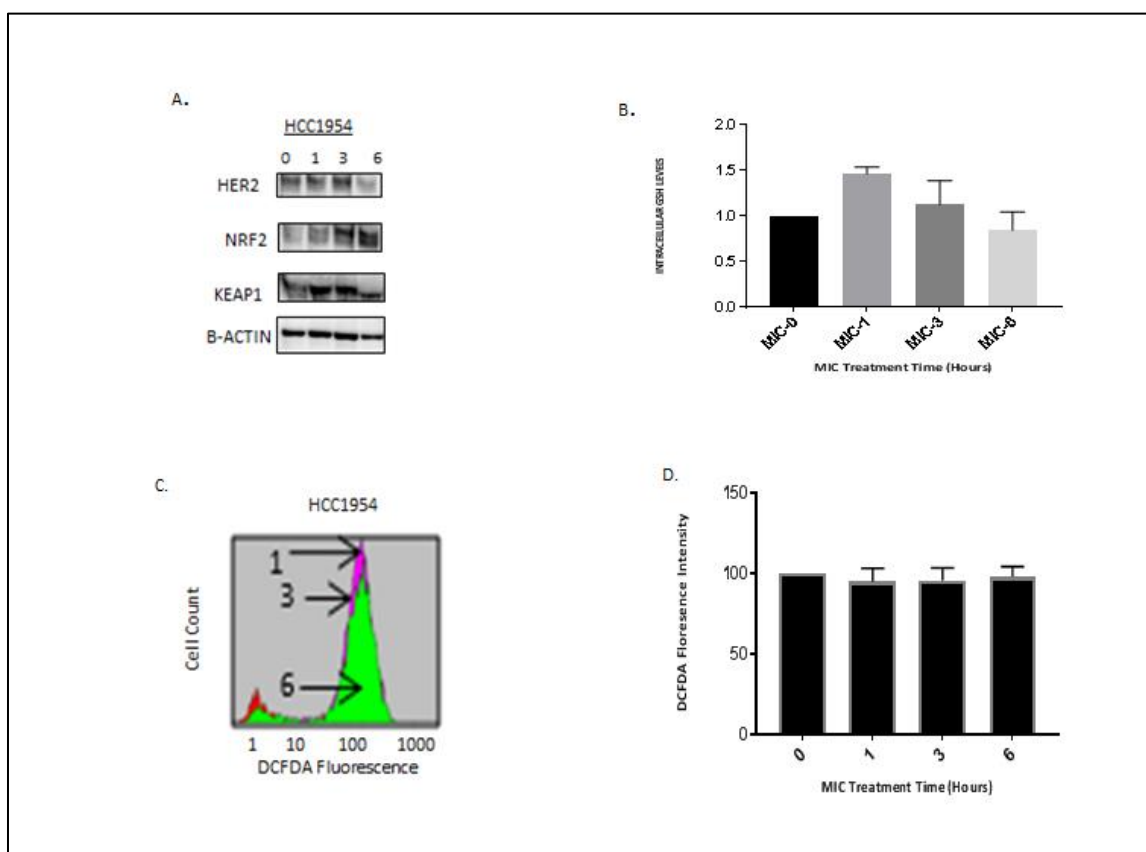
Figure 21: Effect of MIC-1 on HCC1954
  A. Western Blot Analysis of HER2, NRF2, KEAP1, and NQO1 after treatment with 1 μM of MIC-1 and incubation for 1, 3, 6 hours with no MIC-1 treatment labeled as 0
  B. Chart showing changes in ROS levels in response to 1 μM MIC-1 treatment and incubation for 1, 3, 6 hours with no MIC-1 treatment labeled as 0
  C. Histogram showing changes in ROS levels in response to 1 μM MIC treatment and incubation for 1, 3, 6 hours with no MIC-1 treatment labeled as 0
  D. Chart showing changes in GSH levels in response to 1 μM MIC-1 treatment and incubation for 1, 3, 6 hours with no MIC-1 treatment labeled as 0
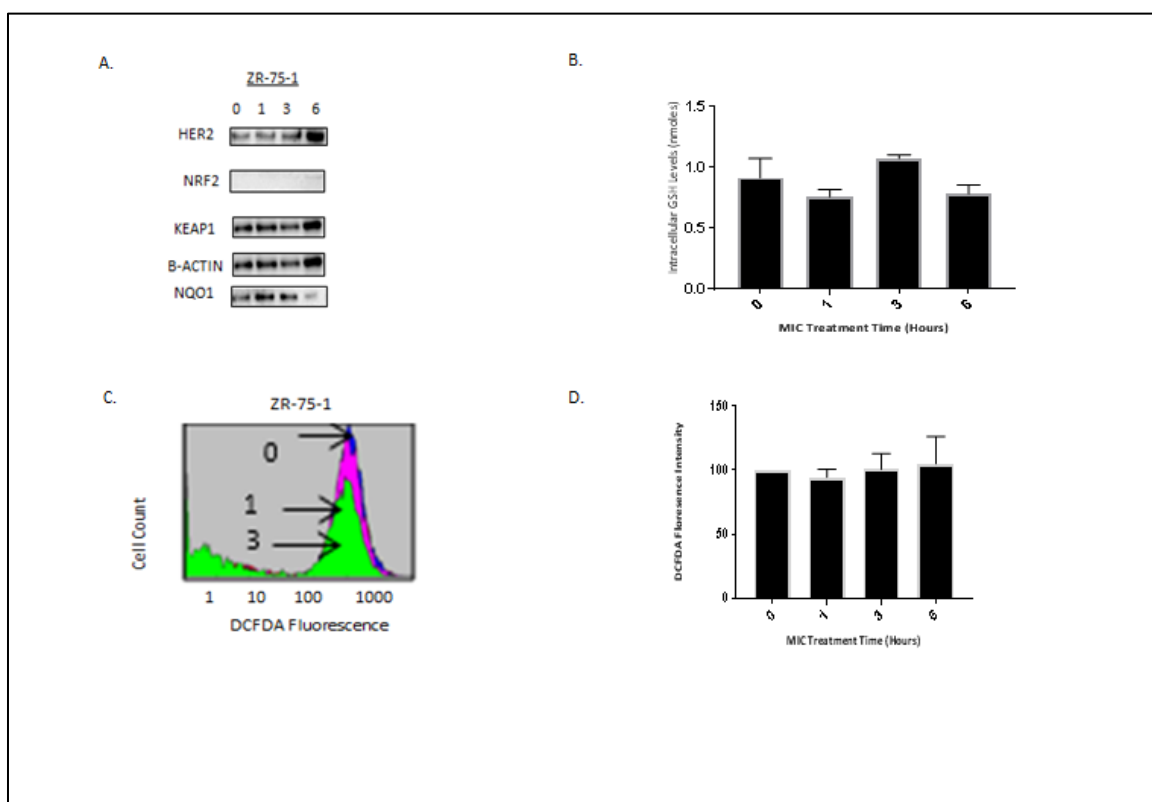
Figure 22: Effect of MIC-1 on ZR75-1
  A. Western Blot Analysis of HER2, NRF2, KEAP1, and NQO1 after treatment with 1 μM of MIC-1 and incubation for 1, 3, 6 hours with no MIC-1 treatment labeled as 0
  B. Chart showing changes in ROS levels in response to 1 μM MIC-1 treatment and incubation for 1, 3, 6 hours with no MIC treatment labeled as 0
  C. Histogram showing changes in ROS levels in response to 1 μM MIC -1treatment and incubation for 1, 3, 6 hours with no MIC treatment labeled as 0
  D. Chart showing changes in GSH levels in response to 1 μM MIC-1 treatment and incubation for 1, 3, 6 hours with no MIC-1 treatment labeled as 0
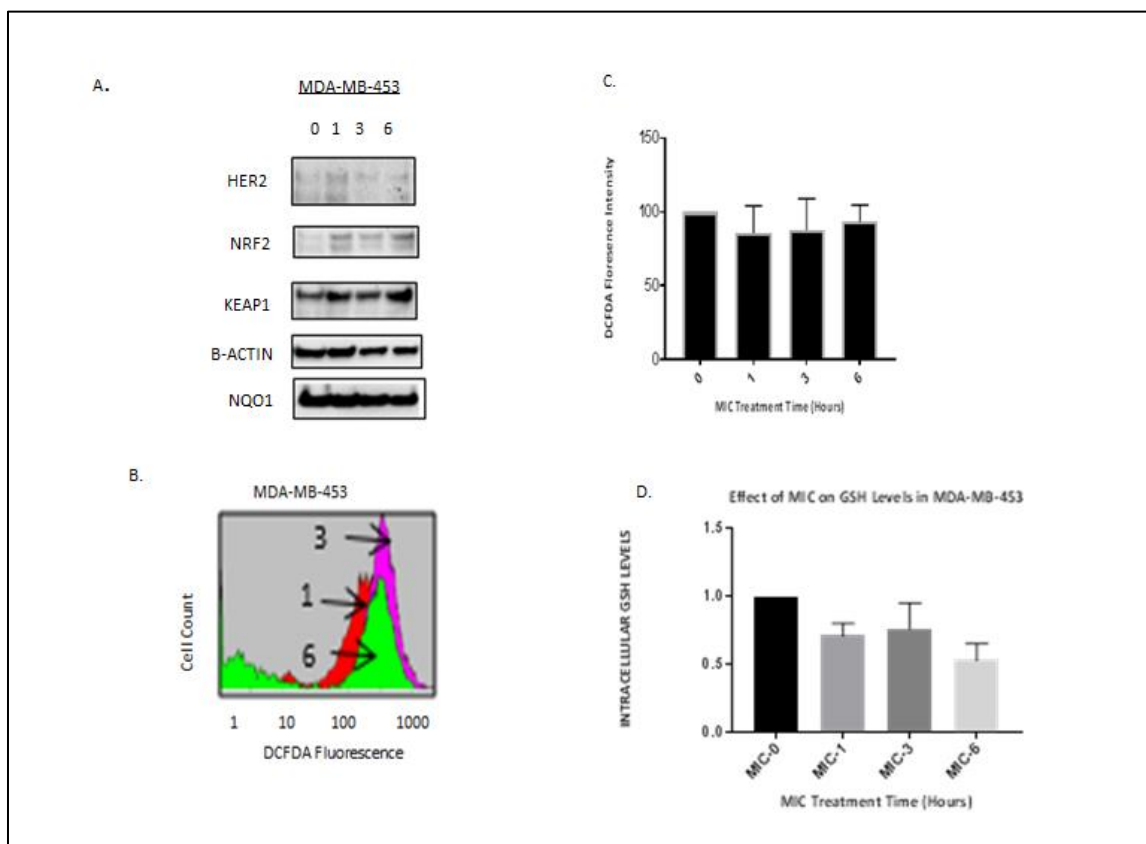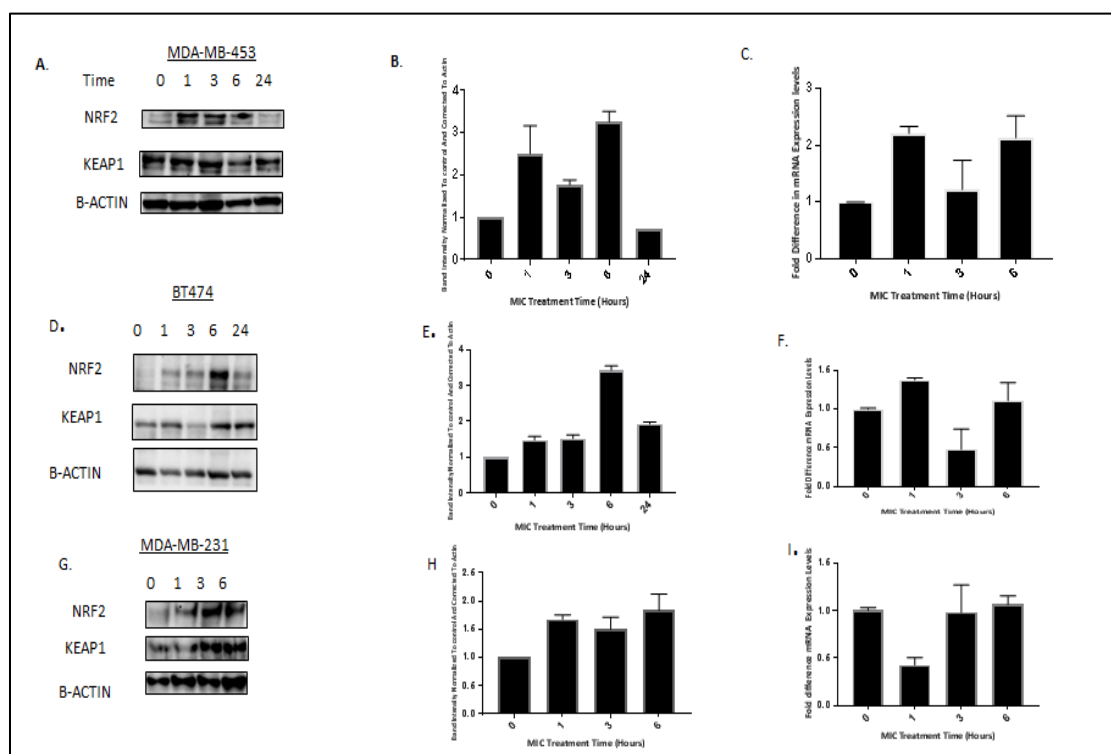
Figure 23: MIC-1 upregulates NRF2 at RNA levels in MDA-MB-231, BT474 and MDA-MB-453

    A. Western Blot Analysis of HER2, NRF2, KEAP1, and NQO1 after treatment with 1 μM of MIC and incubation for 1, 3, 6 hours with no MIC-1 treatment labeled as 0

    B. Chart showing changes in ROS levels in response to 1 μM MIC-1 treatment and incubation for 1, 3, 6 hours with no MIC-1 treatment labeled as 0

    C. Histogram showing changes in ROS levels in response to 1 μM MIC-1 treatment and incubation for 1, 3, 6 hours with no MIC-1 treatment labeled as 0

    D. Chart showing changes in GSH levels in response to 1 μM MIC-1 treatment and incubation for 1, 3, 6 hours with no MIC-1 treatment labeled as 0

3.3.3 MIC Regulates NRF2 at mRNA levels in Breast Cancer Cells

We observed the regulation of NRF2 and KEAP1 expression levels in MDA-MB-453 and MDA-MB 231 cells lines. In some instances, we observed co-upregulation of both NRF2 and KEAP1 in response to MIC-1 treatment. We were curious to know the level at which MIC-1 regulates NRF2 and KEAP1. Our QPCR

results show that MDA-MB-231, MDA-MB-453 and BT474 NRF2 was regulated at the mRNA level.

3.3.4 MIC-1 Triggers Changes in KEAP1 NRF2 interaction

We observed co-upregulation of both NRF2 and KEAP1 in MDA-MB-231 and MDA-MB-453 in response to MIC-1 treatment. Our hypothesis is that MIC-1 triggered a change in KEAP1, which may alter its conformation and its ability to bind properly to NRF2. Or trigger changes that disengage Cul3 ligase such that once NRF2 is bound to KEAP1 it is not degraded hence KEAP1 is perpetually engaged. To test our hypothesis on NRF2 –KEAP1 interaction, we carried out time course experiment using MDA-MB 231 breast cancer cells and a Co-IP to examine the interaction and the effect of 1 µM MIC-1 treatment on the interaction. We observed that there was indeed an interaction between NRF2 and KEAP1, which was maintained during the time course treatment. The presence of the KEAP1 band, which is visible in both the input and the CO-IP lanes in figure 24. If NRF2 is bound to KEAP1 and is not degraded as expected that implies that the protein is not properly bound to KEAP1 or there is a change in KEAP1 that prevents the ubiquitination of NRF2. This was further confirmed in a follow-up experiment, where we transfected MDA-MB-231 with NRF2 before treatment with 1uM MIC for 1 and 3 hours respectively. KEAP1 band was observed which suggest and interaction between NRF2 and KEAP1 which was maintained during treatment with MIC-1 however questions as to the fate of Cul 3 ligase as a result of MIC-1 treatment was not clear and needs to be understood.
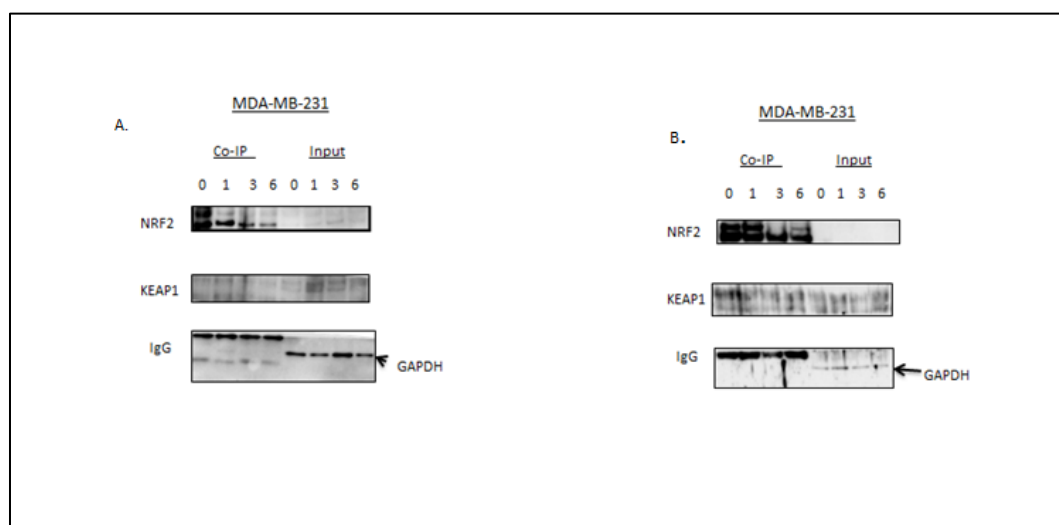
Figure 24: Co-Immunoprecipitation of NRF2 and KEAP1
A& B. Showing NRF2 and KEAP1 pull down. Samples were treated with 1 μM MIC-1 and allowed to incubate for 1, 3 and 6 hours respectively
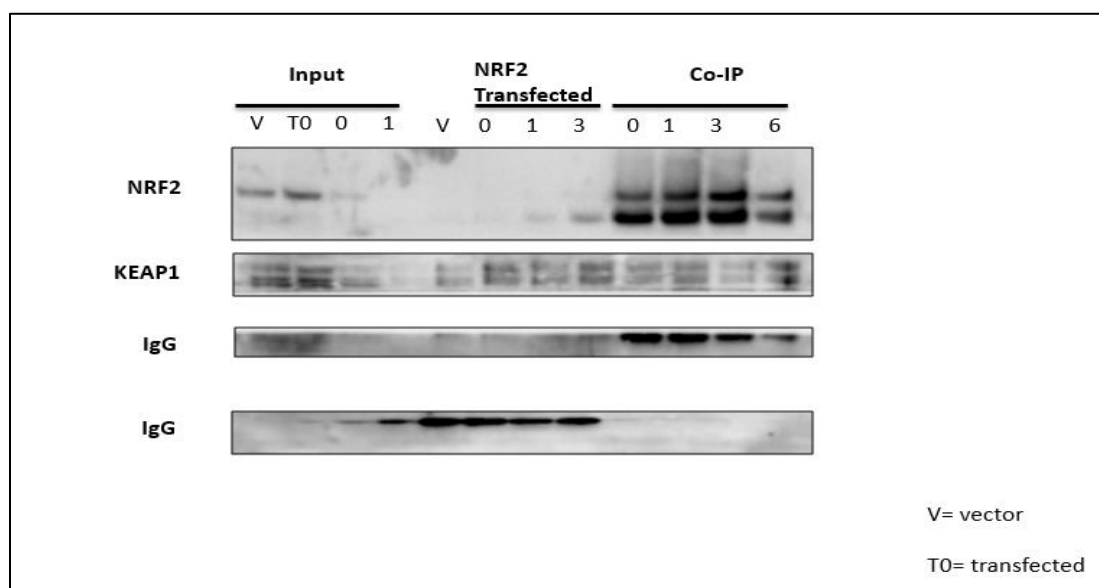
Figure 25 Co-Immunoprecipitation of NRF2 and KEAP1 in MDA-MB-231. Western blot analysis of NRF2 and KEAP1 expression following Co-IP. MDA-MB231 cells were transfected with NRF2 and treated with MIC-1 for 1 and 3 hours respectively before pull down with HA-beads (NRF2 transfected). A transfection control was done using a vector (V) and was not treated with MIC. Endogenous NRF2 pull down was also done after 1uM MIC-1 treatment for 1, 3 and 6 hour treatment respectively.

Conclusion and Future Directions

In this study, we clearly showed that MIC-1 is a potent anti- cancer agent as it inhibited growth of cancer cells across 13 different breast cancer cells lines used. We also showed that MIC is more potent than PEITC another isothiocyanate which is commercially available and has been extensively studied. Our collaborators also reported similar anti-cancer activities in prostate cancer cells (data not shown).

Furthermore, we showed that HER2 overexpression plays a role in hypersensitivity to MIC. Comparing sensitivity of 4 HER2+ breast cancer cells to their HER2- counterparts, we showed that HER2+ cells are more sensitive to MIC than HER2-. Our efforts to understand what is unique to HER2+ cells that may trigger hypersensitivity to MIC led us to discover that ROS levels is higher in HER2+ cells compared to HER2- cells.

Our hypothesis that HER2 overexpression induces hypersensitivity to MIC-1 was proved in our studies using MCF7 and MDA-MB-231 cells overexpressing HER2. MCF7 cells overexpressing HER2 were more sensitive to MIC than the vector expressing cell lines and the same was observed for MDA-MB-231.

This is significant because a positive correlation has been established between HER2 overexpression and poor prognosis in patients.

Changes in intracellular ROS levels in response to MIC-1 varied across the different cell lines. Our results suggest that 1) MIC-1 adopts a ROS mediated pathway in some of the cell lines and 2) MIC-1 mechanism of action varied across the different cell lines.

To understand the mechanism of action of MIC-1 in breast cancer cell lines, we observed changes in KEAP1 and NRF2 in different cell lines in response to MIC-1. In some of the cells we observed co-upregulation of both NRF2 and KEAP1, this suggest that MIC-1 may have triggered some modification to KEAP1, which prevents proper binding of NRF2. Alternatively, modification of KEAP1 in such a way that affects proper Cul3 ligase activity. This improper binding inhibits ubiquitination of NRF2 and later its degradation of NRF2. Our Co-IP results show NRF2 pulled down KEAP1, also, an increase in expression of KEAP1 was even observed with MIC-1 treatment after incubation with 1 μm MIC-1 for 6 hours.

Overall, our results clearly show that HER2 overexpression plays a role in hypersensitivity to MIC-1. Our data also implicates the ROS mediated pathway in MIC-1 mechanism of action.

Further studies employing RNA Sequencing technologies will help identify other pathways triggered by MIC within the cell. Based on the data collected in this study so far, starting with the NRF2-KEAP1 pathway is recommended. In cell-lines where the NRF2 –KEAP1 pathway is regulated by MIC-1 activities, examining genes involved in the apoptotic pathway may be important. This is mainly because, when there is a break down in regulation of ROS, apoptosis may be induced because of the high ROS levels in the cell.

Since the mechanism of action of MIC-1 varies in different cell lines as our data suggested, studies investigating the role of the diverse mutations found in the different cells the MIC-1 mechanism of action will provide valuable information.

The goal of this study is to discover a potential new cancer therapy that may circumvent the challenges associated with existing cancer treatment options. MIC-1 may be useful in treating patients overexpressing HER2, who are resistant to trastuzumab. To properly understand how MIC-1 will perform in vivo, more studies are needed.

Using nude mice, which have compromised immune system, will be valuable for xenograft studies. Studies that will involve introducing breast cancer cells, preferably a HER2+ and HER2- breast cancer cell lines into mice. This will be beneficial in evaluating the efficacy of MIC-1 in vivo and also establish if the sensitivity to MIC-1 is different between HER2+ and HER2- cell in vivo as well. Severe combined immunodeficient (SCID) mice, which have been successfully used for xenograft studies, have defects in T and B-lymphocytes but functional natural killer cells. NOD/SCID, an extreme immunodeficient strain was reported in 1992, is the non-obese diabetic severe immunodeficient mouse. NOD/SCID mouse have significantly reduced activation of natural killer cells and macrophages making this strain a desirable candidate for future studies (121, 122, 123). While immunodeficient mice would be valuable for short-term xenograft study, genetically engineered mouse models (GEMM) can be used for long-term studies.   Through this method we can create homozygous and heterozygous mouse models for the HER2 gene, study the effect of MIC on tumors in vivo and also compare the efficacy of MIC as an anticancer agent to other treatment options currently used today such as trastuzumab. Using such mice models can help detect possible side effect of this treatment.

Chapter 4

Genetic Analysis of Warburg Effect In Yeast

Summary

The Warburg effect describes the increased metabolism of glucose to pyruvate observed in even well oxygenated cancer cells. Even though this phenomenum has been described since 1926, the molecular mechanism is not fully understood. Since a similar phenomenum is observed in yeast described by the Crabtree effect we investigated the underlying mechanism for Warburg in yeast. We proposed that there is an alternate pathway for fatty acid synthesis that bypasses the need for the acetyl coA carboxylase (ACC1) catalyzed synthesis of malonyl CoA. Our studies clearly show that an alternative pathway to producing malonyl CoA may indeed exist yeast cells with genes supressing the *acc1^{cs}* mutant gene.

4.1.1 Introducing Warburg Effect.

Cancer accounts for over 23% of deaths in US alone (111). Due to the prolific

growth that occurs in cancer cells, there is an increased need for biomass and

energy in the cells. This need may be responsible for the changes in cellular

metabolism observed in cancer cells. Changes in different important metabolic

pathway characterize cancer cells (106). In 1956a, Otto Warburg described one of

such changes when he reported a significant increase in glucose uptake by tumor

cells and production of lactic acid under aerobic conditions (known as aerobic

glycolysis). The adoption of this pathway to ATP production could be considered

inefficient since aerobic glycolysis only yields 2 ATP while the normal glycolytic

pathway yields 36 ATP (103). Warburg suggested impaired and irreversible

mitochondrial damage as a reason for aerobic glycolysis a suggestion that had

been refuted by the scientific community (115).

Biochemist Weinhouse, a pioneer in the usage of isotope tracer countered

Warburg's explanation when he reported glucose and fatty acids were oxidized by

cancer cells at comparable levels with normal cells (96), he argued that reduced

mitochondrial activity occurs as a result of elevated glycolytic flux. More studies

have countered the assertion that Warburg effect develops after damage to

oxidative mechanism in the cells. One of such studies geared to determine if

upregulation of glycolysis is a primary response to cellular signaling events or a

response to cellular bioenergetic needs observed more than 90% of glucose carbon was converted to lactate in proliferating primary lymphocytes in response to cytokine signals (97). It has also been noted that percentage ATP produced per glucose molecule if glycolytic flux is high enough may exceed the amount of ATP produced via oxidative pathway (98)

The underlying reason for Warburg effect is not fully understood, aerobic glycolysis as explained by Warburg in 1926, aligned well with Pasteur's postulations in 1861. Pasteur observed that glycolysis is upregulated in yeast under hypoxic conditions. Similar to Warburg effect, the Crabtree effect that describes the fermentation of glucose as a preferred metabolic pathway instead of respiration in yeast. Unlike the Warburg effect, the Crabtree effect is a reversible reaction while Warburg effect is not. With comparable metabolic processes occurring in both yeast and cancer cells, we were able to tap into the power of yeast genetics to explore fatty acid synthesis during aerobic glycolysis
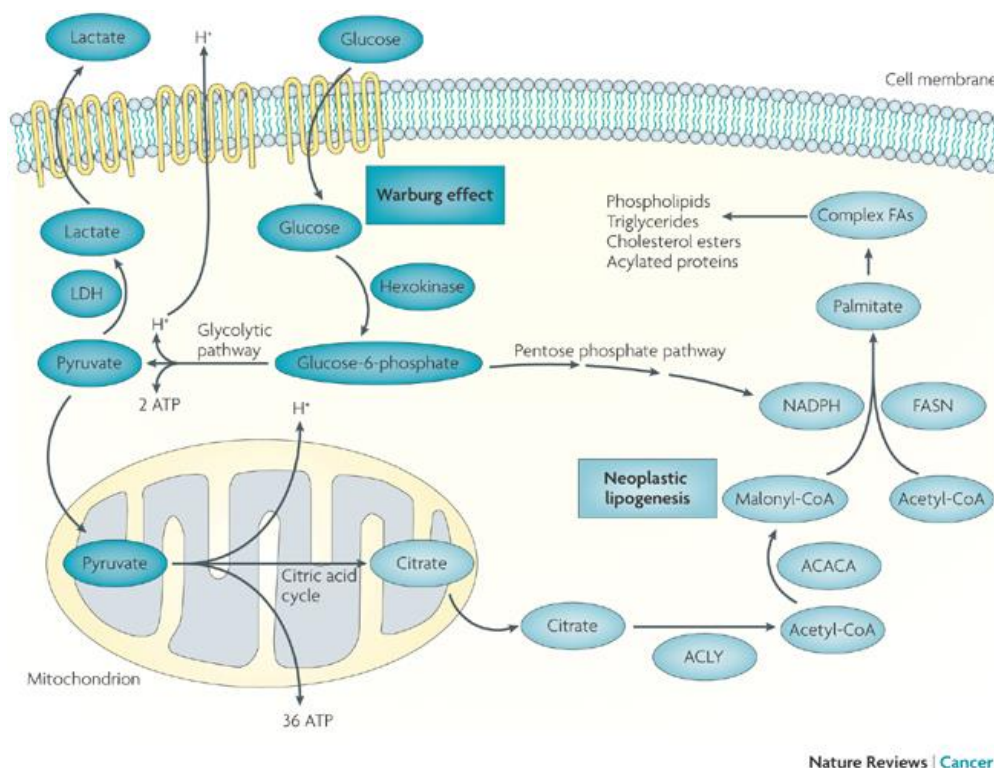
Figure 26 : **Fatty acid synthesis and glucose metabolism and connected in cancer cells**. It shows that as pyruvate is generated, a product of the glycolytic pathway, it is converted to acetyl CoA. Acetyl CoA enters the citric acid cycle in the mitochondria where citrate is produced, the citrate produced can either be oxidized to generate ATP or exported out to the cytoplasm where it is converted back to acetyl CoA in a reaction catalyzed by ATP citrate lyase, acetyl CoA produced can then enter into the fatty acid synthesis pathway. *Source: Menendez, J.A. and R. Lupu (2007). Fatty acid synthase and lipogenic phenotype in cancer pathogenesis. Nature reviews, Cancer. Vol 7: 765*

4.1.2 Fatty acid Synthesis and Cancer

Key players in the fatty acid synthesis pathway have been implicated in cancer cell proliferation. In 1994, Kuhajda and collegues noticed an elevated amount of a substance called OA-519 in cancer cells with poor prognosis; they later found out that OA-519 is fatty acid synthase

 In normal cells de novo fatty acid synthesis is suppressed and fatty acid for cellular activity is obtained from diet/ exogenous sources, since fatty acid synthesis is suppressed in normal cells, expression of fatty acid synthase in normal cells is very low (117). Studies also showed inhibiting citrate lyase (an important enzyme linking glucose metabolism to fatty acid synthesis) using siRNA suppressed tumor growth (107). Knocking down Acetyl CoA carboxylase alpha using RNAi has also been shown to result in a decrease in lipogenesis and cell apoptosis induction in cancer cells (102). These studies and several other studies point to the importance of understanding the fatty acid synthesis pathway and the potential it holds for effective treatment options.

4.1.3: Fatty Acid Synthesis in Normal Cells

Fatty acid synthesis is an important source of energy, and essential for cell membrane formation along with other cellular functions. In normal cells, the first step in fatty acid synthesis that is also the rate-limiting step is the carboxylation of acetyl CoA to malonyl CoA. This highly regulated and irreversible step is catalyzed by the enzyme acetyl CoA carboxylase. The synthesis of malonyl CoA is followed by a sequence of reactions (condensation, reduction, dehydration and reduction)which results in elongation of the fatty acid chain (101). Out of 25 enzymes involved in fatty acid synthesis, 3 are crucial to the main pathway (116). The 3 crucial enzymes are : (1) acetyl CoA carboxylase (ACC) which catalyzes the synthesis of Malonyl CoA from acetyl CoA, (2) citrate lyase which catalyzes the synthesis of acetyl CoA from citrate. 3) Fatty acid synthase, which catalyzes the condensation of malonyl CoA and acetyl CoA to produce palmitic acid (105).

4.1.4: Key Players in Cellular Metabolic Pathway

α-keto acids are naturally occurring amino acids that play crucial roles in cellular metabolism. Pyruvate, a 3-carbon compound and oxaloacetate a 4 carbon compound are examples of α-keto acids (118). Also important to cellular metabolism are some α-keto dehydrogenase complexes such as pyruvate dehydrogenase complex (PDC), which catalyzes the decarboxylation of pyruvate to form acetyl CoA (113).

Pyruvate + CoA + NAD^+ → Acetyl COA + CO_2 + NADH + H^+

PDC has two important catalytic subunits, dihydrolipoamide acetyltransferase (E2) and dihydrolipoamide dehydrogenase (E3) . E2 has a dual function, catalytic and structural function (110), while E3 function in electron transfer from NAD+ forming NADH (113).

Another α-keto dehydrogenase complex important to this study is α-keto glutarate dehydrogenase complex (KGDC) which unlike PDC does not have the E2 subunit but does have the E3 subunit. KGDC catalyzes the formation of succinyl COA from α-ketoglutarate a 5 carbon compound.

α-ketoglutarate + CoA + NAD^+ $\longrightarrow$ succinyl-CoA + HCO_3^- + NADH + H^+
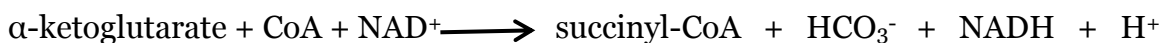
(Adapted from Olayanju et al 2015)

While there are dehydrogenase complexes catalyzing the decarboxylation of 3 carbon compounds (pyruvate) and 5 carbon compounds (α-ketoglutarate), no

dehydrogenase complex has been reported for 4 carbon compounds in eukaryotes. This is one of the underlying basis of this study.

The hypothesis for this study was built on the following: (I) As of the time of this study, no 4-carbon dehydrogenase complex has been reported in eukaryotes. (II) The existence of a 4-carbon dehydrogenase would catalyze malonyl CoA synthesis through an alternative pathway, bypassing the need for ACC1 (III) The substrate for this 4 carbon dehydrogenase catalyzed reaction, oxaloacetate is readily available in the cell, produced from pyruvate in a reaction catalyzed by pyruvate carboxylase (99).

We hypothesize that a new enzymatic activity may have emerged in cancer cells that allow cells to bypass the need for the ACC1 catalyzed step in fatty acid synthesis. Specifically, we propose that a mutation may have occurred in either PDC or KGDC, because of the mutation these enzymes lose their substrate specificity and allow a 4-C substrate instead of their normal substrate. This new enzymatic activity will also come with respiratory impairment.

$$\text{Oxaloacetate} + \text{CoA} + \text{NAD}^+ \longrightarrow \boxed{\text{MaCoA}} + \text{HCO}_3^- + \text{NADH} + \text{H}^+ \quad \text{(Adapted}$$
from Olayanju et al 2015)
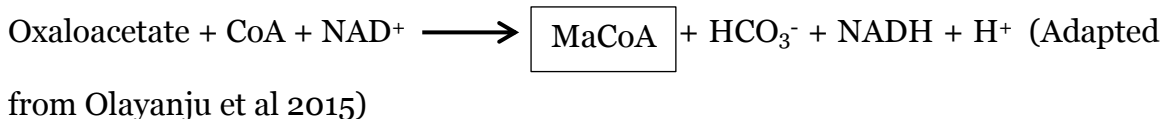
4.1.5 Precedence For Emergence of Catalytic Activity

There has been precedence for the emergence of a new catalytic activity as a result of a mutation. In the work by Cantley and colleagues, they showed that a

mutation in isocitrate dehydrogenase gene resulted in the loss of substrate specificity for isocitrate. The reaction that catalyzes the formation of α-ketoglutarate from isocitrate was disrupted by this mutation and a new enzymatic activity emerged catalyzing the formation of 2- hydroxyglutarate (2HG) from α-ketoglutarate (100).

Figure 27 : Structural Analysis of R132H Mutant: a) R132H IDH1 active site with α-ketoglutarate (yellow) embedded. This image shows the change in conformation of the active site of the enzyme due to the R to H change at position 132. b) The wild-type IDH1 active site with the normal substrate isocitrate (yellow) and NADP (grey). Adapted from L Dang *et al. Nature* **000**, 1-6 (2009)
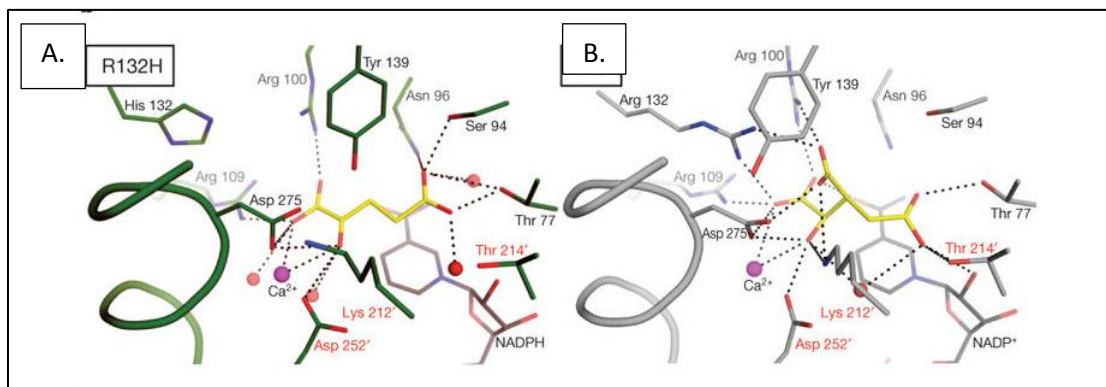
4.2 Experimental Approach

4.2.1 Isolation and genetic analysis of acc1^{cs} suppressors

Yeast strain H470 used in this study was a generous gift from Dr. Steve Brill at Rutgers University. The wild type yeast strain W303 and opposite mating time strain YMH 1341 was from the Hampsey lab stock.

H470 is a cold sensitive *acc1^{cs}* mutant, which evolved as a result of a missense mutation in Acc1 (G1783A) (112). Due to this mutation there is impaired Acc1 activity and malonyl CoA depletion at restrictive temperatures hence cells fails to grow at 16^e C (Csm$^-$ phenotype)

We **isolated 53 spontaneous suppressors** of this Csm$^-$ phenotype, 51 of which failed to respire (measured by inability to grow on 3% glycerol as the only carbon source, Gly$^-$ phenotype), only 2 suppressors were respiratory competent. These suppressors, which were assigned different R numbers, have pleiotropic phenotypes, which are desirable for cloning purposes. The primary mutant carries a mutation for the ade2-1 allele; hence, the Ade2 deficiency is also of interest in this study. Mutants, which are defective for the ade2-1 allele, form red colonies which results from AIR accumulation. The suppressors are predominantly white, while only a few turned pink, this is consistent with our hypothesis. Respiratory defect along with the suppression of the Csm- phenotype is also consistent with our hypothesis, where we predicted that synthesis of malonyl CoA through an alternate pathway bypassing the need for ACC1 comes with respiratory impairment. After backcrossing the suppressors to *acc1^{cs}* mutants (YMH 1341), the diploids grow at 16^e C suggesting that exhibit a

dominant gain of function mutation with regards to malonyl CoA synthesis and also failed to respire, (recessive for Gly⁻).

4.2.2 Gene Determination.

 Complementation Test: To identify the gene responsible for the suppression of *acc1ᶜˢ* we carried out complementation tests using pda1Δ , pdb1Δ and kgd1Δ deletion mutants, this categorized our 51 mutants into 3 complementation groups. These results indicate that these strains have alleles of pda1 (R34, R38, R41, R56) (figure 28), pdb1 (R3, R34, R36, R47, R49, R64) (figure 27) and kgd1 (R46, R61, R92, R96)(figure 28).

Figure 28: Diploids (H470 revertants x *pda1Δ*). Plates on the left were grown on YPD while the plates on the right were grown on YPG; both sets were grown at 30°C. Cells that fail to be complemented by *pda1Δ* deletion strains when glycerol is the only carbon source are suppressors of *pda1Δ* allele
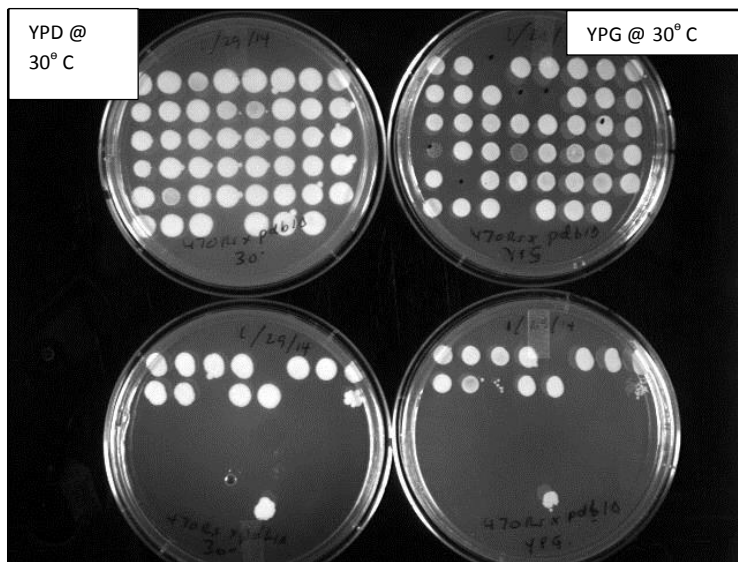
Figure 29: Diploids (H470 revertants x *pdb1Δ*). Plates on the left were grown on YPD while the plates on the right were grown on YPG; both sets were grown at 30°C. Cells that fail to be complemented by *pdb1Δ* deletion strains when glycerol is the only carbon source are suppressors *of pdb1Δ* allele

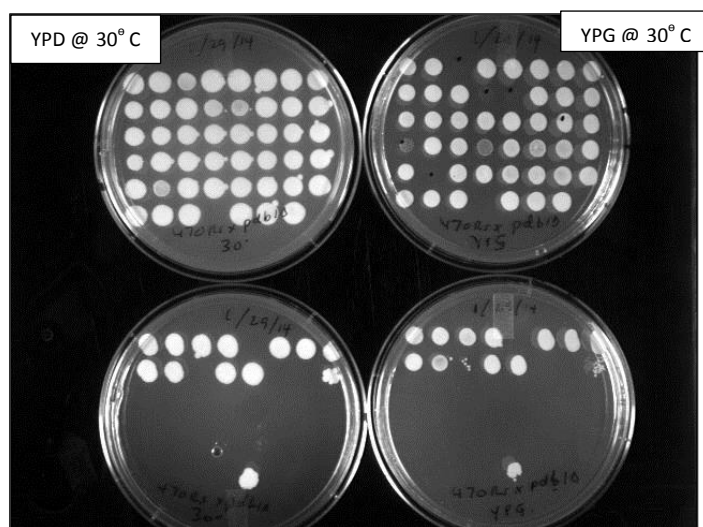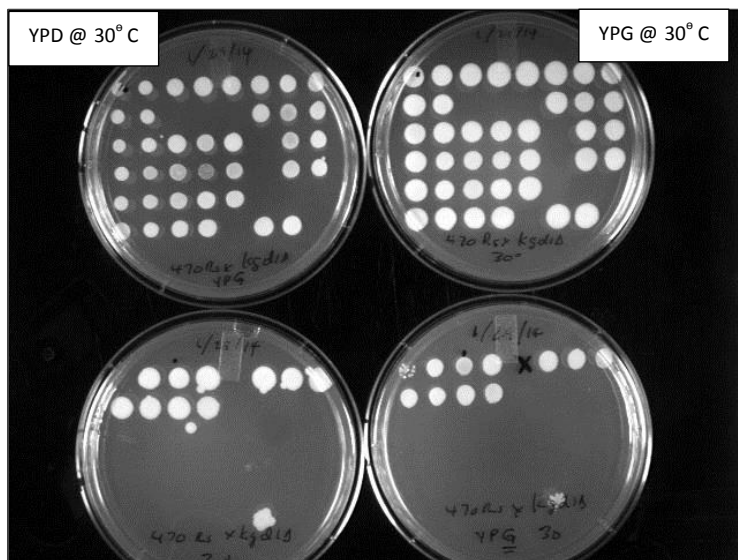**Figure 30**: **Diploids (H470 revertants x *kgd1Δ*).** Top: Plates on the left were grown on YPG while the plates on the right were grown on YPD; both sets were grown at 30°C. Bottom: plates on the left were grown on YPD while the plates on the right were grown on YPG. Cells that fail to be complemented by *kgd1Δ* deletion strains when glycerol is the only carbon source are suppressors of *kgd1Δ* allele
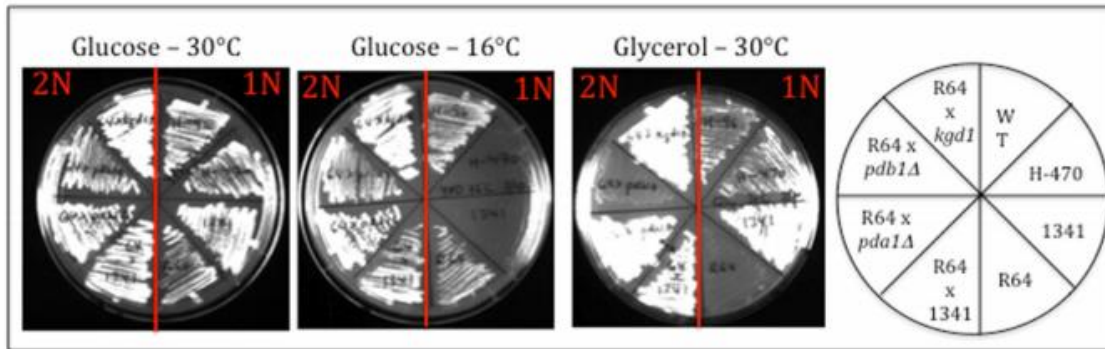
Figure 31: Growth phenotypes for the R64 suppressor of acc1 cs . The right panel depicts growth of strains on 2% glucose medium at 30°C (2 days); the middle panel depicts growth on 2% glucose at 16°C (10 days); the right panel depicts growth on 3% glycerol medium (3 days). The red lines divide diploid (2N) and haploid (1N) strains. Key: WT (ACC1 +); H-470 (MATα acc1 cs); 1341 (MATa acc1 cs); R64 (acc1 cs pdb1 sup). Adapted from Olayanju et al Adv. Biol Regul. 2015

4.2.3 Cloning: This result of the complementation test was further confirmed

by introducing plasmid borne wildtype copies of PDA1, PDB1 and KGD1 to the

acc1^{cs} suppressors. Since the plasmid carried a LEU2 marker, selection after

transformation was carried out on a –leu plate. Transformants were screened for

ability to respire, a phenotype accessed by the ability to grow on YPG plates

(plates with glycerol as the only carbon source).

Out of the 51 *acc1^{cs}* suppressors used in this study 2 suppressors which we named

R34 and R64 showed distinct restoration of respiratory efficiency by ability to

grow on –Leu +Gly plates after transformation with PDA1 and PDB1 carrying

plasmids respectively (Figure 32)
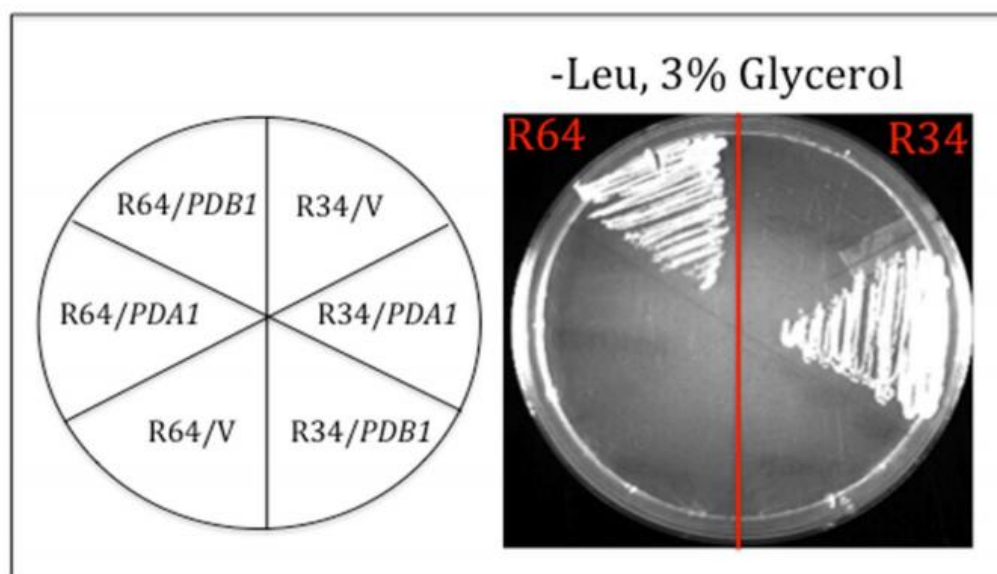
Figure 32: Complementation results for *acc1^cs* suppressors R34 and R64 Showing growth for each strain with either PDA1 or PDB1. Selection of transformants was carried out on – Leu, 2% glucose medium, then scored respiratory competence on –Leu, 3% glycerol medium. Image was acquired after two days incubation at 30°C. Adapted from Olayanju et al.2015

4.2.4 Suppressors of *acc1^cs* Resistant To Soraphen Toxicity

Soraphen has been shown to inhibit and also deplete the cell of Malonyl CoA (Schneiter et al., 2000). H470 *acc1^cs* mutant, which grows at 30° C, fails to grow at this temperature in the presence of 250 nM of Soraphen. If indeed our hypothesis is true that *acc1^cs* suppressors produce malonyl CoA through an alternative pathway, bypassing the need for acc1 then our suppressors should be able to resist Soraphen A and grow in the presence of Soraphen A. Here we report that 14 of our *acc1^cs* suppressors are resistant to Soraphen A, this was observed at 1000 nM concentration (Figure 33). A concentration 4 times the concentration that prevented growth of the *acc1^cs* mutant.
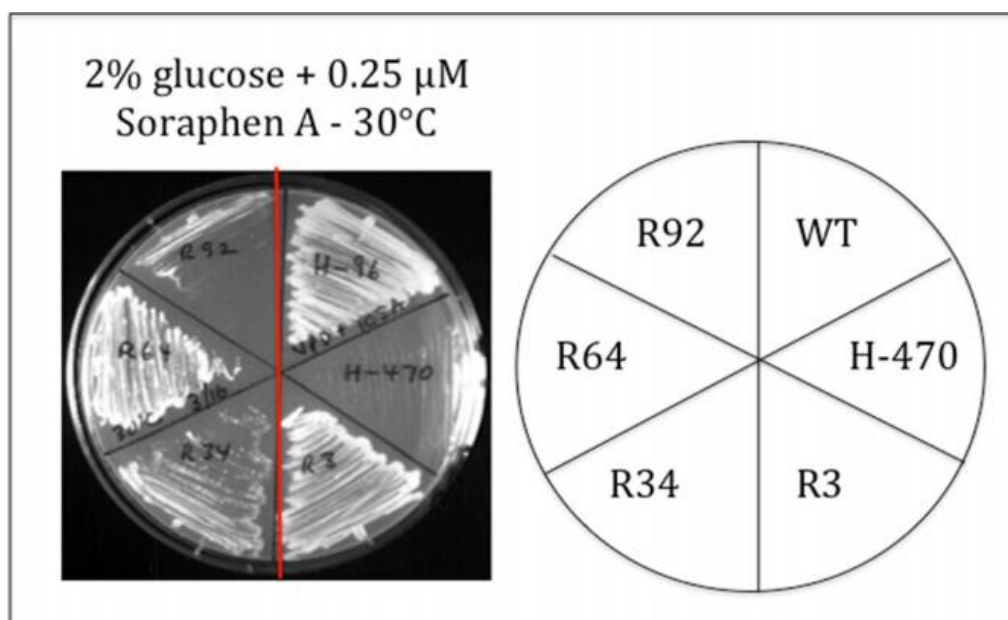
Figure 33: **Resistance to Soraphen A Toxicity:** Here we show that H470 (*acc1ᶜˢ* mutant) is sensitive to Soraphen A (an inhibitor of ACC1). The growth defect observed in H470 is suppressed by *acc1ᶜˢ* suppressors, this was all done at 30ᵉ C. Adapted from Olayanju et al 2015

4.2.5 Increase in Fatty Acid Synthesis Observed in *acc1ᶜˢ* suppressors

Fatty acid content in *acc1ᶜˢ* mutant, different *acc1ᶜˢ* suppressors was evaluated by staining the cells with Nile red (9-diethylamino-5H-benzo [α] phenoxazine-5-one), an established assay for fatty acid levels. Nile red fluorescence intensity under fluorescence microscope varies with amount of fatty acid in the cell. Our data shows higher fluorescence in Nile red intensity in *acc1ᶜˢ* suppressors when compared to wildtype and mutants. (Figure 34)
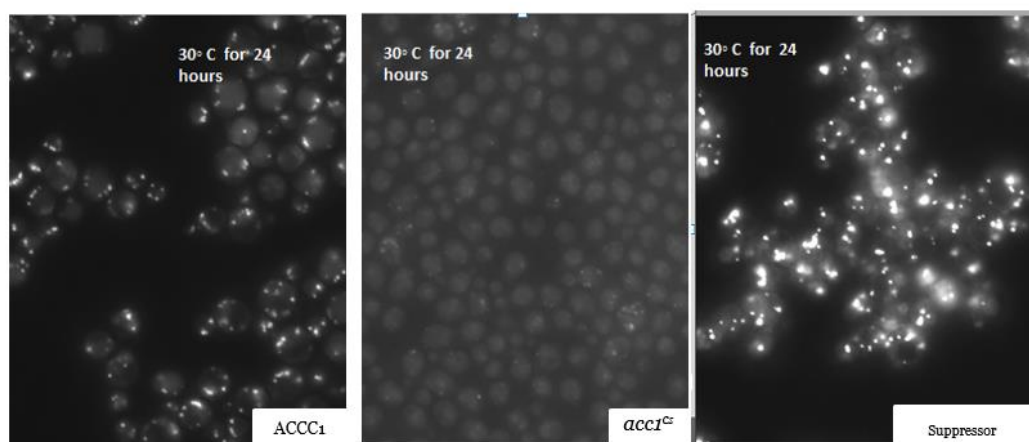
Figure 34: **Comparison of Fatty Acid Content of wildtype**, *acc1cs* mutants and *acc1cs* suppressors. Cells were stained with Nile red and allowed to incubate for 24 hours at 30° C before the images above were taken.

4.3 Conclusion and Future Directions

Our work clearly shows that a mutation exist that confers the ability to produce fatty acid inspite the mutation or inhibition of the acc1 gene. Employing an unbiased genetic approach, we isolated 53 spontaneous *acc1^cs* suppressors, 51 of which were respiratory incompetent based on their inability to grow on a medium with glycerol as the main carbon source.

We hypothesized that a mutation may have occurred in subunits of pyruvate dehydrogenase complex PDA1 and PDB1 changing the conformation of the active site along with its substrate specificity. Our complementation analysis showed that our *acc1^cs* suppressors complemented either pda1, pdb1 or α-ketoglutarate dehydrogenase (kgdc). We proposed that if indeed there is an alternate pathway to malonyl CoA synthesis that bypasses the need for ACC1 then malonyl CoA will still be produced inspite of ACC1 inhibition. Our studies using Soraphen A (a potent inhibitor of ACC1) showed that *acc1^cs* suppressor indeed produce malonyl CoA despite ACC1 inhibition. An upregulation of fatty acid synthesis was also observed in *acc1^cs* suppressors compared to *acc1^cs* mutants and suppressors.

We also showed higher fatty acid content in *acc1^cs* suppressors as compared to *acc1^cs* mutants or wildtype. Soraphen A was unable to inhibit the growth of *acc1^cs* suppressors either unlike *acc1^cs* mutants whose growth was inhibited by 250 nM of Soraphen. Identifying a mutation unique to cancer cells is of great importance, as this unique mutation will provide a target for cancer therapeutics with minimal side effects.

Whole genome sequencing comparing genome for ACC1, *acc1^cs* suppressors and *acc1^cs* mutants will provide information on the different genes that may play roles

in the phenotypes observed in the different categories of interest and also shed light of possible genetic interactions that may play roles *acc1cs* suppressor phenotype.

References

1. Al-Asmari AK, Albalawi SM, Athar MT, Khan AQ, Al-Shahrani H, Islam M. Moringa oleifera as an anti-cancer agent against breast and colorectal cancer cell lines. PloS ONE. 2015; 10: e0135814

2. Anderson ME, and Meister A. Transport and direct utilization of y-glutamylcyst(e)ine for glutathione synthesis. Proc. N&Z. Acad. Sci. USA 1983; 80: 707-711.

3. Ambrosone CB, McCann SE, Freudenheim JL, Marshall JR, Zhang Y, Shields PG. Breast cancer risk in premenopausal women is inversely associated with consumption of broccoli, a source of isothiocyanates, but is not modified by GST genotype. J Nutr. 2004; 134:1134–1138.

4. Bannai S. Transport of cysteine and cysteine in mammalian cells. Biochim. Biophys. Acta 1984; 779: 289-306.

5. Barba FJ, Nikmaram N, Roohinejad S, Khelfa A, Zhu Z, Koubaa M. Bioavailability of Glucosinolates and Their Breakdown Products: Impact of Processing. Front Nutr. 2016; 3:24.

6. Berkovich L, Earon G, Ron I, Rimmon A, Vexler A, Lev-Ari S. *Moringa oleifera* aqueous leaf extract down-regulates nuclear factor-kappaB and increases cytotoxic effect of chemotherapy in pancreatic cancer cells. BMC Complement. Altern. Med. 2013; 13, pp. 212-219

7. Boggs DA, Palmer JR, Wise LA, Spiegelman D, Stampfer MJ, Adams-Campbell LL, Rosenberg L. Fruit and vegetable intake in relation to risk of breast cancer in the Black Women's Health Study. Am J Epidemiol. 2010; 172:1268–1279. doi: 10.1093/aje/kwq293.

8. Boone JJ, Bhosle J, Tilby MJ, Hartley JA, Hochhauser D. Involvement of the HER2 pathway in repair of DNA damage produced by chemotherapeutic agents. Mol Cancer Ther. 2009 Nov; 8(11):3015-23.

9. Boreddy SR, Pramanik KC, Srivastava SK. Pancreatic tumor suppression by benzyl isothiocyanate is associated with inhibition of PI3K/AKT/FOXO pathway. Clinical Cancer Research. 2011; 17:1784–1795.

10. Burk RF, Patel K, and Lane JM. Reduced glutathione protection against rat liver microsomal injury by carbon tetrachloride-dependence on 02. Biochem. J. 1983; 215: 441-445,

11. Chausseaud LF. The role **of** glutathione and glutathiqne Stransferases in the metabolism **of** chemical carcinogens and other electrophilic agents. Adv Cancer Res. **29:175–274**

12. Cho HS, Mason K, Ramyar KX, Stanley AM, Gabelli SB, Denney DW, et al. Structure of the extracellular region of HER2 alone and in complex with the Herceptin Fab. Nature. 2003

13. Connor MJ, and Wheeler LA. Depletion of cutaneous glutathione by ultraviolet radiation. Photochem. PhotobioZ. 1987; 46: 239-245.

14. DeLucia AJ, Mustafa M, Hussain Z, and Cross CE. Ozone interaction with rodent lung. III. Oxidation of reduced glutathione and formation of mixed disulfides between protein and nonprotein sulfhydryls. J. CZin. Invest. 1975; 55: 794-802,

15. Divi SM, Bellamkonda R, Dasireddy SK. Evaluation of antidiabetic and antihyperlipedemic potential of aqueous extract of *MO* in fructose fed insulin resistant and STZ induced diabetic wistar rats: a comparative study Asian J. Pharm. Clin. Res. 2012; 5 :67-72

16. Doroshow JH. Doxorubicin-induced cardiac toxicity. New Engl J Med. 1991; 324: 843-845.

17. Ekerljung L, Lindborg M, Gedda L, Frejd FY, Carlsson J. Dimeric HER2-specific affibody molecules inhibit proliferation of the SKBR-3 breast cancer cell line. Biochem Biophys Res Commun. 2008.

18. Fahey JW, Zalcmann AT, Talalay P. The chemical diversity and distribution of glucosinolates and isothiocyanates among plants. Phytochemistry. 2001; 56(1):5-51.

19. Fariss MW, and Reed DJ. Measurement of glutathione and glutathione disulfide efflux from isolated rat hepatocytes. In: Isolation, Characterization, and Use of Hepatocytes. New York: Elsevier. 1983; 349

20. Federico A, Morgillo F, Tuccillo C, Ciardiello F, Loguercio C. Chronic inflammation and oxidative stress in human carcinogenesis. Int J Cancer J Int Du Cancer. 2007; 121:2381–6

21. Fowke JH, Chung FL, Jin F, Qi D, Cai Q, Conaway C, Cheng JR, Shu XO, Gao YT, Zheng W. Urinary isothiocyanate levels, brassica, and human breast cancer. Cancer Res. 2003; 63:3980–3986.

22. Fukushige S, Matsubara K, Yoshida M, Sasaki M, Suzuki T, Semba K, Toyoshima K, Yamamoto T. Localization of a novel v-erbB-related gene, c-

erbB-2, on human chromosome 17 and its amplification in a gastric cancer cell line. Mol Cell Biol. 1986; 6: 955-958.

23. Furukawa T, Meydani SN, and Blumerg JB. Reversal of age-associated decline in immune responsiveness by dietary glutathione supplementation in mice. Mech. Ageing Dev. 1987; 38: 107- 117.

24. Gao N, Budhraja A, Cheng S, Liu EH, Chen J, Yang Z, Chen D, Zhang Z, Shi X. Phenethyl isothiocyanate exhibits antileukemic activity in vitro and in vivo by inactivation of Akt and activation of JNK pathways. Cell Death & Disease. 2011;2:e140

25. Garrett TP, McKern NM, Lou M, Elleman TC, Adams TE, Lovrecz GO, et al. The crystal structure of a truncated ErbB2 ectodomain reveals an active conformation, poised to interact with other ErbB receptors. Mol Cell. 2003; 11:495–505

26. Gopalakrishnan L. Doriya K. Kumara D.S. *Moringa Oleifera*: A review on nutritive importance and its medical application. Food Science and Human Wellness, 2016 ;5 :2

27. Gupta P. and Srivastava, SK. Antitumor activity of phenylethyl isothiocyanate in HER2- positive breast cancer models. BMC Medicine. 2012; 10:80

28. Hagen TM, Aw TY, and Jones DP. Glutathione uptake and protection against oxidative injury in isolated kidney cells. Kidney Int. 1988; 34: 74-81.

29. Hagen TM, Brown LA, and Jones DP. Protection against paraquat-induced injury by exogenous GSH in pulmonary alveolar type II cells. Biochem. Pharmacol. 1986; 35: 4537-4542.

30. Halliwell B, Gutteridge J. Free radicals in biology and medicine. 4th ed. Oxford University Press; 2007

31. Halkier BA, Gershenzon J. Biology and biochemistry of glucosinolates. Annu Rev Plant Biol . 2006; 57:303–33.

32. He X, Chen MG, Lin GX, Ma Q. Arsenic induces NAD(P)H-quinone oxidoreductase I by disrupting the Nrf2•Keap1•Cul3 complex and recruiting Nrf2•Maf to the antioxidant response element enhancer. J. Biol. Chem. 2006; 281:23620–31

33. Horie T, Ono K, Nishi H, Nagao K, Kinoshita M, Watanabe S, Kuwabara Y, Nakashima Y, Takanabe-Mori R, Nishi E, Hasegawa K, Kita T, Kimura T. Acute doxorubicin cardiotoxicity is associated with miR-146a-induced

inhibition of the neuregulin-ErbB pathway. Cardiovasc Res. 2010; 87: 656-664.

34. Itoh K, Chiba T, Takahashi S, Ishii T, Igarashi K, Katoh Y, Oyake T, Hayashi N, Satoh K, Hatayama I, Yamamoto M, Nabeshima Y. An Nrf2/small Maf heterodimer mediates the induction of phase II detoxifying enzyme genes through antioxidant response elements. Biochem Biophys Res Commun. 1997 Jul 18;236 (2):313-22.

35. Jenkinson SG, Black RD, and Lawrence RA. Glutathione concentrations in rat lung bronchoalveolar lavage fluid: effects of hyperoxia. J. Lab. CZin. Med. 1988; 112: 345-351.

36. Jenkinson SG, Marcum RF, Pickard JS, Orzechowski Z, Lawrence RA, and Jordan JM. Glutathione disulfide formation occurring during hypoxia and re-oxygenation of rat lung. J. Lab. CZin. Med. 1988; 112: 471-480.

37. Jones DP. Radical-free biology of oxidative stress. Am J Physiol Cell Physiol. 2008;4:C849–68.
38. Kansanen E, Kuosmanen SM, Leinonen H, and Anna-Liisa L. The Keap1-Nrf2 pathway: Mechanisms of activation and dysregulation in cancer. Redox Biol. 2013; 1(1): 45–49.

39. Kasolo JN, Bimenya GS, Ojok L, Ochieng L, Ogwal-okeng JW (2010). Phytochemicals and uses of *MO* leaves in Ugandan rural communities J. Med. Plants Res. 2010; pp. 753-757

40. Keum YS. Regulation of the Keap1/Nrf2 system by chemopreventive sulforaphane: implications of posttranslational modifications. Ann N Y Acad Sci. 2011 Jul;1229:184-9

41. Kosower NS, Kosower EM. The Glutathione Status of Cells International Review of Cytology Volume 54, 1978, Pages 109-160

42. Kraus MH, Issing W, Miki T, Popescu NC, Aaronson SA. Isolation and characterization of ERBB3, a third member of the ERBB/epidermal growth factor receptor family: evidence for overexpression in a subset of human mammary tumors. Proc Natl Acad Sci USA. 1989;86:9193–9197

43. King CR, Kraus MH, Aaronson SA. Amplification of a novel v-erbB-related gene in a human mammary carcinoma. Science. 1985; 229: 974-976. 10.1126/science.2992089

44. Kobayashi A, Kang MI, Okawa H, Ohtsuji M, Zenke Y, et al. Oxidative stress sensor Keap1 functions as an adaptor for Cul3-based E3 ligase to regulate proteasomal degradation of Nrf2. Mol. Cell. Biol. 2004; 24:7130–39.

45. Lacenere CJ, Sternberg PW. Regulation of EGF receptor signaling in the fruitfly D. melanogaster and the nematode C. elegans. Breast Dis. 2000; 11:19–30.

46. Lee-Hoeflich ST, Crocker L, Yao E, Pham T, Munroe X, Hoeflich KP, Sliwkowski MX, Stern HM. A central role for HER3 in HER2-amplified breast cancer: implications for targeted therapy. Cancer Res. 2008 Jul 15;68(14):5878-87.

47. Loganathan S. Kandala PK, Gupta P, Srivastava SK. Inhibition of EGFR-AKT axis results in the suppression of ovarian tumors in vitro and in preclinical mouse model. PLoS One. 2012;7:e43577

48. Li X, Zhang D, Hannink M, Beamer LJ. Crystal structure of the Kelch domain of human Keap1. J. Biol. Chem. 2004;279:54750–58

49. Mbikay M. Therapeutic potential of *MO* leaves in chronic hyperglycemia and dyslipidemia: a review Front. Pharmacol. 2012; pp. 1-12

50. Meister A. On the cycles of glutathione metabolism and transport. In: Current Topics in Cellular Regulation. New York: Academic, 1982; vol. 10, p. 21-58.

51. Meister A, and Anderson M. Glutathione. Annu. Reu. Biochem. 1983; 52: 711-760

52. Miller AC and Henderson BW. The influence of cellular glutathione content on cell survival following photodynamic treatment in vitro. Radiat. Res. 1986; 107: 83-94,

53. Mitchell JB, Russo A, Kinsella J and Glatstein E. Glutathione elevation during thermotolerance induction and thermosensitization by glutathione depletion. Cancer Res. 1983; 43: 987- 991.

54. Moghal N, Sternberg PW. The epidermal growth factor system in Caenorhabditis elegans. Exp Cell Res. 2003; 284:150–159.

55. Ogura T, Tong KI, Mio K, Maruyama Y, Kurokawa H, et al. Keap1 is a forked-stem dimer structure with two large spheres enclosing the intervening, double glycine repeat, and C-terminal domains. Proc. Natl. Acad. Sci. USA. 2010; 107:2842–47.

56. Padmanabhan B. Tong KI, Ohta T, Nakamura Y, Scharlock M, et al. Structural basis for defects of Keap1 activity provoked by its point mutations in lung cancer. Mol. Cell. 2006; 21:689–700.

57. Palmer S. Diet, nutrition, and cancer. Prog Food Nutr Sci. 1985; 9: 283-341.

58. Parker CW, Fischman CM, and Wedner HJ. Relationship of biosynthesis of slow reacting substance to intracellular glutathione concentrations. Proc. NatZ. Acad. Sci. USA. 1980; 77: 6870- 6873.

59. Primiano T, Sutter TR, and Kensler TW. Antioxidant Inducible Genes. Adv. Pharm. 1997; 38, 293-3282

60. Reed DJ. Defense mechanisms of normal and tumor cells. J. RadioZ. Oncol. 1986; 12: 1457-1461.

61. Richman PG, and Meister A. Regulation of y-glutamylcysteine synthetase by nonallosteric feedback inhibition by glutathione. J. BioZ. Chem 1975; 250: 1422-1426

62. Robiquet PJ, and Boutron F. Sur la semence de moutarde. J. Pharm. Chim. . 1831; 17, 279–282

63. Sahu RP, Srivastava SK. The role of STAT-3 in the induction of apoptosis in pancreatic cancer cells by benzyl isothiocyanate. Journal of the National Cancer Institute. 2009;101:176–193

64. Scaltriti M, Rojo F, Ocaña A, et al. Expression of p95HER2, a truncated form of the HER2 receptor, and response to anti-HER2 therapies in breast cancer. *Journal of the National Cancer Institute*. 2007; 99(8):628–638.

65. Semba K, Kamata N, Toyoshima K, Yamamoto T. A v-erbB-related protooncogene, c-erbB-2, is distinct from the c-erbB-1/epidermal growth factor-receptor gene and is amplified in a human salivary gland adenocarcinoma. Proc Natl Acad Sci USA. 1985; 82: 6497-6501.

66. Sierke SL, Cheng K, Kim HH, Koland JG. Biochemical characterization of the protein tyrosine kinase homology domain of the ErbB3 (HER3) receptor protein. Biochemical Journal. 1997; 322:757–763

67. Shaw JP, and Chou IN. Elevation of intracellular glutathione content associated with mitogenic stimulation of quiescent fibroblasts. J. CeZZ. Physiol. 1986; 129: 193-198.

68. Shapiro TA, Fahey JW, Wade KL, Stephenson KK, Talalay P. Human metabolism and excretion of cancer chemoprotective glucosinolates and isothiocyanates of cruciferous vegetables. Cancer Epidemiol Biomarkers Prev. 1998 Dec;7(12):1091-100.

69. Shih C, et al. Transforming genes of carcinomas and neuoblastomas introduced into mouse fibroblast. Nature. 1981; 290, 261

70. Slamon DJ, Clark GM, Wong SG, Levin WJ, Ullrich A, McGuire WL. Human breast cancer: correlation of relapse and survival with amplification of the HER2/neu oncogene. Science. 1987; 235: 177-182. 10.1126/science.3798106

71. Sliwkowski MX, Mellman I. Antibody therapeutics in cancer. Science. 2013 Sep 13;341(6151):1192-8.

72. Sønderby, IE, et al. Biosynthesis of glucosinolates – gene discovery and beyond. Trends Plant Sci. 2010; 15, 283–290

73. Rajan et al. Anticancer activity of glucomoringin isothiocyanate in human malignant astrocytoma cells. **Fitoterapia** 2016; Volume 110, Pages 1-7

74. Taguchi K, Motohashi H, Yamamoto M. Molecular mechanisms of the Keap1–Nrf2 pathway in stress response and cancer evolution.

75. Tong KI, Katoh Y, Kusunoki H, Itoh K, Tanaka T, Yamamoto M. Keap1 recruits Neh2 through binding to ETGE and DLG motifs: characterization of the two-site molecular recognition model. Mol. Cell. Biol. 2006; 26:2887–900

76. Trachootham D, Zhou Y, Zhang H, Demizu Y, Chen Z, Pelicano H, Chiao PJ, Achanta G, Arlinghaus RB, Liu J, Huang P. Selective killing of oncogenically transformed cells through a ROS-mediated mechanism by beta-phenylethyl isothiocyanate. Cancer Cell. 2006 Sep;10(3):241-52.

77. Wang X, Di Pasqua AJ, Govind S, McCracken E, Hong C, Mi L, Mao Y, Wu JY, Tomita Y, Woodrick JC, Fine RL, Chung FL. Selective depletion of mutant p53 by cancer chemopreventive isothiocyanates and their structure-activity relationships. J Med Chem. 2011.

78. Warin R, Xiao D, Arlotti JA, Bommareddy A, Singh SV. Inhibition of human breast cancer xenograft growth by cruciferous vegetable constituent benzyl isothiocyanate. Mol Carcinog 2010; 49:500–7.

79. Waterman C, Rojas-Silva P, Tumer TB, et al. Isothiocyanate-rich *Moringa oleifera* extract reduces weight gain, insulin resistance, and hepatic gluconeogenesis in mice. Mol Nutr Food Res. 2015; 59:1013–1024.

80. Waterman C, Cheng DM, Rojas-Silva P, Poulev A, Dreifus J, Lila MA, Raskin I. Stable, water extractable isothiocyanates from Moringa

oleifera leaves attenuate inflammation in vitro. Phytochemistry. 2014 Jul;103:114-122.

81. Wattenberg LW. Inhibition of carcinogenesis by minor anutrient constituents of the diet. Proc Nutr Soc. 1990; 49: 173-183.

82. Weitberg AB, Weitzman SA, Clark EP, and Stossel TP. Effects of antioxidants on oxidant-induced sister chromatid exchange formation. J. CZin. Invest. 1985; 75: 1835-1841.

83. Xiao D. Srivastava SK, Lew KL, Zeng Y, Hershberger P, Johnson CS, Trump DL, Singh SV. Allyl isothiocyanate, a constituent of cruciferous vegetables, inhibits proliferation of human prostate cancer cells by causing G2/M arrest and inducing apoptosis. Carcinogenesis. 2003; 24:891–897.

84. Zhang Y, et al. A major inducer of anticarcinogenic protective enzymes from broccoli: isolation and elucidation of structure. Proc. Natl. Acad. Sci. 1992; 89, 2399–2403.

85. Yoon-Hee H, Hafiz U, Untek J, Boyun K, Jiyoung S, Dong HS, and Yong-Sang S. ROS Accumulation by PEITC Selectively Kills Ovarian Cancer Cells via UPR-Mediated Apoptosis Front Oncol. 2015;5:167.

86. Yokota J, Yamamoto T, Toyoshima K, Terada M, Sugimura T, Battifora H, Cline MJ. Amplification of c-erbB-2 oncogene in human adenocarcinomas in vivo. Lancet. 1986; 1: 765-767.

87. Yoneda T, Williams PJ, Hiraga T, Niewolna M, Nishimura RA. Bone-Seeking Clone Exhibits Different Biological Properties from the MDA-MB-231 Parental Human Breast Cancer Cells and a Brain-Seeking Clone In Vivo and In Vitro. Journal of Bone and Mineral Research. 2001.

88. Youjin K, Wu AG, Jaja-Chimedza A, Graf BL, Waterman C, Verzi MP, Raskin I. Isothiocyanate-enriched moringa seed extract alleviates ulcerative colitis symptoms in mice. Plos One 2017.

89. Zhang D.D. Lo S.C. Cross J.V. Templeton D.J. Hannink M. Keap1 is a redox-regulated substrate adaptor protein for a Cul3-dependent ubiquitin ligase complex. Mol. Cell. Biol. 2004;24: 10941.

90. Burgess AW, Cho HW, Eigenbrot C, Ferguson KM, Thomas PJ, Garrett - Leahy D L, Lemmon MA, Sliwkowski MX, Ward CW, Yokoyama S. An Open-and-Shut Case? Recent Insights into the Activation of EGF/ErbB Receptors. Molecular Cell Volume 12, Issue 3, 2003, Pages 541-552.

91. Barnes CJ, Kumar R. Biology of the epidermal growth factor receptor family. Cancer Treat Res. 2004; 119:1–13.

92. Prenzel N, Fischer OM, Streit S, Hart S, Ullrich A. The epidermal growth factor receptor family as a central element for cellular signal transduction and diversification. Endocr Relat Cancer. 2001; 8:11–31.

93. Bazley LA, Gullick WJ. The epidermal growth factor receptor family. Endocr Relat Cancer. 2005; 12 (Suppl 1): S17–S27.

94. Yarden Y, Sliwkowski MX. Untangling the ErbB signalling network. Nat Rev Mol Cell Biol. 2001;2:127–137.

95. Shin L, et al. NRF2 Modulates Aryl Hydrocarbon Receptor Signaling: Influence on Adipogenesis Mol. Cell. Biol. October 2007vol. 27 no. 20 7188-7197.

96. Weinhouse S, Millington RH, Wenner CE. Metabolism of neoplastic tissue. I. The oxidation of carbohydrate and fatty acids in transplanted tumors. Cancer Res. 1951; 11:845–50.

97. Bauer DE, Harris MH, Plas DR, Lum JJ, Hammerman PS, Rathmell JL, Riley CB, et al. Cytokine stimulation of aerobic glycolysis in hematopoietic cells exceeds proliferative demand FASEB J., 18 (2004), pp. 1303-1305

98. Guppy M, Greiner E, Brand K. The role of the Crabtree effect and an endogenous fuel in the energy metabolism of resting and proliferating thymocytes Eur. J. Biochem., 212 (1993), pp. 95-99

99. Patra KC, Hay N. The pentose pathway and cancer. Trends in biochemical sciences. 2014 39: 347-354

100. Dang L, White DW, Gross S, Bennet BD, Bittinger MA, Driggers EM, Fatin VR, Jang HG, et al Cancer associated IDH1 mutations produce 2 hydroxyglutarate Nature 2009:462: 739-744

101. Berg JM, Tymoczko JL, Stryer L. Biochemistry. 5th edition. New York: W H Freeman; 2002. Section 22.4, Fatty Acids Are Synthesized and Degraded by Different Pathways. Book: http://www.ncbi.nlm.nih.gov/books/NBK22554/

102. Chajes V, Cambot M, Moreau K, Lenoir GM, and Joulin V. Acetyl CoA carboxylase α is essential to breast cancer survival. Cancer Res (2006); 66(10).

103. Costello LC, and Franklin RB. Why do tumor cells glycolyse? From glycolysis through citrate to lipogenesis. Mol Cell. Biochem(2005). 280, 1-8

104. Deberardinis RJ, Lum JJ, Hatzivassiliou G, Thompson CB. The Biology of Cancer: Metabolic Reprogramming Fuels Cell Growth and Proliferation Cell Metab. 7, 11 (2008).

105. Goodridge AG. Fatty acid synthesis in eukaryotes. Amsterdam: Elsevier Science (1991).

106. Hanahan D, Weinberg RA. Hallmarks of cancer: the next generation, Cell (2011)144: 646-647.

107. Hatzivassiliou et al. ATP citrate lyase inhibition can suppress tumor cell growth. Cancer cell (2005); 8, 311-321.

108. Kuhajda FP, Jenner K, Wood FD, et al. Fatty acid synthesis: a potential selective target for antineoplastic therapy. Proc Natl Acad Sci USA (1994).. 91: 6379

109. Kuhajda FP. Fatty acid synthase and human cancer: new perspectives on its role in tumor biology. Nutrition (2000)16, 202-208.

110. Oliver RM, Reed LJ. Multienzyme complexes. In electron microscopy of proteins. Academic Press 1982; Vol. 2:1-48.

111. Preetha AA, Kunnumakara B, Kuzhuvelil CS, Harikumar B, Lai OS, Sung B, and Aggarwal BB . Cancer is a Preventable Disease that Requires Major Lifestyle Changes. Pharm Res. (2008) ; 25(9): 2097–2116.

112. Schneiter R. Guerra CE, Lampl M, Tatzer V, Zellnig G, Klein HL, and Kohlwein SD. A novel cold sensitive allele of the rate-limiting enzyme of fatty acid synthesis, acetyl co A carboxylase, affects the morphology of yeast vacuole through acylation of Vac8p. Molecular and cellular biology (2000)20, 2984-2995.

113. Thekkumkara TJ, Pons G, Mitroo S, Jentoft JE, and Patel MS. Molecular biology of human pyruvate dehydrogenase complex: structural aspects of E2 and E3 components. Annals of New York Academy of Science (1989); 113-129

114. Warburg O. On respiratory impairment in cancer cells. Science 1956a

115. Warburg O. Origin of Cancer cells. Science (1956);123, 309-314.

116. Watson JA, Fang M, Lowenstein JM. Tricarballylate and hydroxycitrate: substrate and inhibitor of ATP: citrate oxaloacetate lyase. Arch Biochem Biophy, (1969);135:209–17.

117. Weiss L, Hoffman G, Schreiber R, et al. Fatty acid biosynthesis in man, a pathway of minor importance. Biol Chem (1986) 367:905-912

118. Walkil SJ. Structure and function of animal fatty acid synthase. Lipids (2004); 39, 1045-1053.

119. Jung IL. Soluble Extract From Moringa oleifera leaves with a New Anti-cancer activity. PLOS ONE 2014 ; Vol 9

120. Klapper LN, Waterman H, Sela M, Yarden Y. Tumor-inhibitory antibodies to HER-2/ErbB-2 may act by recruiting c-Cbl and enhancing ubiquitination of HER-2. Cancer Res. 2000 Jul 1; 60(13):3384-8.

121. Bosma GC, Custer RP, Bosma MJ. A severe combined immunodeficiency mutation in the mouse. Nature. 1983;301(5900):527-530

122. Prochazka M, Gaskin HR, Shultz LD, et al. The nonobese diabetic scid mouse: model for spontaneous thymomagenesis associated immunodeficiency mutation in the mouse. Pro Natl Aca Sci USA 1992;89(8) 3290-3294.

123. Shultz LD, Schweitzer PA, Christianson SW et al. Multiple defects in innate and adaptive immunologic function in NOD/LtSz-scid mice. J Immunol. 1995; 154(1): 180-191.